



Eidgenössische Technische Hochschule Zürich
Swiss Federal Institute of Technology Zurich

Machining Optical Cavities on Optical Fibers and Substrates

Summer project

Huang, Guanhao

September 19, 2017

Advisors: Prof. Jonathan Home
Dr. Klara Theophilo
Simon Ragg

Department of Physics, ETH Zürich

Abstract

We have set up an automatic laser ablation platform for producing concave mirrors on optical fibers and substrates to create cavities that have very small size, waist, mode volume and high finesse. In this report the backgrounds of this research area is discussed and the fabrication method of our setup is discribed. We discuss the cavity parameters we are aiming, then show how to manufacture fiber-based Fabry-Perot cavities (FFPCs) using photonic crystal fibers (PCF) with single-shot ablation, multi-shot ablation and laser polishing methods. We also planned applied similar methods to substrates but got no time. The outcomes were examined by both interferometry imaging and AFM check, and achieved what we were expecting.

Acknowledgement

Jonathan Home for giving me this precious opportunity of conducting an internship in his group.

Mirjam Bruttin for administrative support.

Klara Theophilo for providing literatures, setup components design and purchasing, theory support and thesis revising.

Simon Ragg for helping me do the AFM check.

Atac Imamoglu for allowing us to use and modify their setup for laser ablation.

Thomas Flint for introducing their setup and providing the Python subscript to analyze the surface.

All the other group members for helping me whenever I turned to them.

Contents

Contents	v
1 Introduction	1
1.1 Background	1
1.2 Fiber-based Fabry-Perot Cavity	2
1.2.1 Single-shot laser machining	2
1.2.2 Multi-shot laser machining	3
1.3 Photonic crystal fibers	4
1.4 Substrates	4
1.5 Polishing pulse	5
1.6 Cavity and coupling parameters	6
1.6.1 Definition and optical parameters	6
1.6.2 Waist radius	6
1.6.3 Fiber coupling	7
1.7 Ablation process	9
2 Fabrication	11
2.1 Optical setup	11
2.2 Fiber preparation	14
2.2.1 Collapsing	14
2.2.2 Splicing	17
2.2.3 Ablation simulation	20
2.3 Ablation procedure	22
2.4 Surface analysis	25
2.4.1 Interferometric surface analysis	25
2.4.2 AFM surface analysis	26
2.5 Fiber coating	28
3 summary	31

A Appendix	33
A.1 Beam propagating calculation	33
A.1.1 Mode radius calculation	33
A.1.2 Coupling efficiency with respect to the cavity parameters	34
A.2 Instruction for the program	34
A.3 Python codes used	37
A.3.1 To analyze the fiber tip surface	37
A.3.2 To determine the position of the core (quick but rough)	39
A.3.3 To determine the position of the core (slow but accurate)	40
A.3.4 To determine the size of the field beam (normal fibers)	42
Bibliography	47

Introduction

1.1 Background

Obtaining strong coupling between atoms and photons is interesting for many quantum information communities like trapped ions. As the ion-light interface could be associated with most of the qubit state preparation, control and readout in a trapped ion system, one provides strong light-matter coupling and easy optical access is needed. Also, it shall make us closer for scalable quantum processors and networks of photons connecting trapped ion registers.[10] Efforts have been made to build such elementary quantum network using single neutral atoms with cavities[16]. One similar way to build the network using trapped ion systems is to integrate optical cavities with ion traps in vacuum.

For a single two-level atom at the antinode of the cavity mode, the cooperativity could be enhanced as $\eta = 2(F/\pi)(\frac{3}{2\pi}\lambda_0^2)/(\frac{1}{2}\pi\omega^2)$, where F is the finesse of the cavity and ω is the mode waist which is proportional to the distance from the ion to the optical element[19]. Integrating an ion trap with a compatible cavity requires high finesse and close distance while avoiding disturbance of the trapping electric fields, thus improving the overall performance of the system[3].

To make it compatible with the trapped ion system, several implementations[3] of micro-cavities have been pursued, trying to miniaturize the cavities and at the same time maintain a high cavity finesse.

Fiber cavities are one promising type. First it allows access to smaller mode volumes than macroscopic mirrors. Also, when the photons exit the cavity, they directly get coupled into the fiber and further reduce the loss. Additionally, fibers are more flexible to be installed in various setups than macroscopic mirrors. Actually, fiber-based-cavities integrated ion trap has already been implemented[3], but suffered from fiber charging.

Several groups have tried many methods to get fine mirror surface and suitable geometric features to be able to get high performance[9, 18, 14]. The

methods developed from single shot to multi-shots while rotating the fiber. In our setup we first implement the single shot method at an early stage of the experiment. Then, we upgrade our setup to move to the rotating approach to further optimize the surface structure.

After pursuing fiber cavities, we didn't have time to produce substrate concave mirrors. The guy who is to take over my work is encouraged to further explore the possibilities.

1.2 Fiber-based Fabry-Perot Cavity

To be compatible with scalable quantum information processing systems, a fiber-based Fabry-Perot cavity (FFPC) that is miniaturized and still maintaining a high finesse is a good candidate. The essential part for the FFPC is the concave mirrors on the tip of the fibers with ultralow roughness and high quality coating, while having the suitable geometry for particular system. A cavity is formed when two of these fiber tips oppose to each other. It is not a new idea of creating mirrors on the tip of the fiber. Many implementations have been tried but the finesse they achieved is relatively moderate[9]. The method we are to implement of fabricating a mirror on the tip of the fiber using CO₂ laser pulses to shape the concave mirror surface is capable of reaching relatively high finesse with an order of 10^5 . The method was first invented in [9]. The reason to choose CO₂ laser is that the vibrational mode of silica has a strong absorption of CO₂ laser radiation[5], so the ablation of fiber tip surface is made possible.

1.2.1 Single-shot laser machining

Our first attempt to produce a fine concave mirror on the tip of a single mode fiber is the following: Using CO₂ laser pulse in pulsed regime to send a single shot to ablate the fiber tip surface. In this way a smooth surface in Gaussian shape is formed[9]. Afterwards, high-reflective dielectric coating is applied to turn the facet into a mirror. The fiber is first cleaved nicely, and then we apply a pulse within certain parameter regime to ablate the surface. The surface gets ablated and melting occurs in a thin layer to smooth the surface. When the ablation happens within the first several microns of the tip surface, the depth is approximately proportional to the light intensity. Thus, a Gaussian profile is expected. The structure of the surface created could be controlled by the pulse duration, power and waist. Using this method we could machine structure with radius of curvature within a certain range and at the same time control the roughness of the surface. The method is first used to generate concave shape with small radius of curvature at the order of tens of microns, but could also be implemented to generate the ones with hundreds of microns. Thus, a small waist of mode is acquired and a high

cooperativity is able to be achieved. The types of cavities with ROC of tens of microns and small cavity distance is preferred by neutral atoms experiments as they do not disturb the trapping potential while provide a small mode volume. But for ions, they are likely to disturb the trapping potential if the cavity length is too short[3]. By using cavities with larger distance which requires larger ROC, we would expect to see less coupling efficiency.

1.2.2 Multi-shot laser machining

In the previous section fibers were machined by a single shot laser pulse. But due to the laser beam profile does not necessarily be perfect gaussian profile due to astigmatism which could possibly cause an elliptical concave profile. The consequence of having an elliptical concave profile is that the cavity will exhibit significant birefringence which were actually observed in some previous researches trying to install cavity to an ion trap[3]. This will obstruct their application in some experiments involving polarization superpositions. It also couples higher order modes that decrease the finesse of the cavity[1]. Further more, applying a focused single shot laser usually results in small radius of curvature of the concave mirror and small diameter. The fiber cavity manufactured this way will suffer from the limited cavity length due to the clipping loss at the edge of the indentation. In some applications, like the coupling of atomic ions to a fiber cavity, due to the potential disturbance of the trapping electric field caused by the presence of the fiber, a relatively long cavity length is desired. Our cavity-integrated-trap design is shown in figure 1.1. The distance between the two cavity mirrors is about $400\mu m$ limited by the trap size itself.

Thus, this method of multi-shot ablation procedure is invented to both reduce the ellipticity of the mirror and allows a longer cavity length[18]. The main idea is to apply pulses with longer duration and lower intensity with larger waist so that each pulse shall have a moderate impact on the surface while affecting a bigger diameter. To have a bigger diameter is to prevent clipping at the mirror as a larger cavity distance would result in larger mode on the mirror. And after certain number of moderate pulses we rotate the fiber for a certain angle (90°) and apply the pulses again. We continue the procedure until a full round is completed. By doing the rotation we could reduce the asymmetry of the concave mirror we produce. And by applying multiple moderate pulses it is more easier for us to control the radius of curvature to be longer than before. However, the main motivation for applying this multi-shot laser machining method is to reduce the birefringence, since finesse is observed to be largely determined by the coating quality[9].

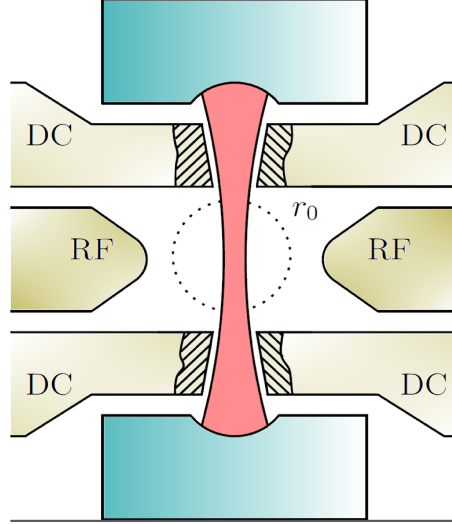


Figure 1.1: Our cavity-integrated ion trap design.

1.3 Photonic crystal fibers

We planned to build fiber-based Fabry-Perot cavities using photonic crystal fibers (PCFs) LMA-25. This type of fibers already have a wide range of applications. They provide lower optical transmission loss and higher damage thresholds than conventional fibers[11]. These fibers are constructed by drawing pure silica to create a cross section with several air holes which you can see in figure 1.2. What interests us is that LMA-25 has a relatively larger core, with a big mode field radius of about $10.2\mu m$, which is near to the cavity mode field radius on the cavity mirror under our configuration. In this case our fiber coupling efficiency is optimized. You can find detailed calculation in section 1.6.3. Additionally, the PCFs won't exhibit the ridge in the mirror profile as mentioned by other experiments[18] which might cause a major decrease of the cavity finesse.

1.4 Substrates

The FFPCs described above have already been implemented by several groups. The fiber-based cavity system, however, has bad mode matching efficiency between the fiber propagating mode and cavity mode, especially when the radius of curvature is below $10\mu m$. For fiber-based cavity with a radius

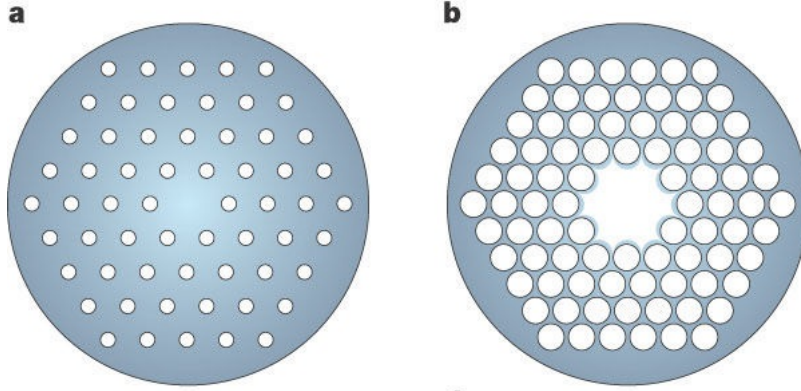


Figure 1.2: PCF with a pure silica core surrounded by a reduced-index photonic crystal cladding material, a image taken from [11]. **a** shows a silica core and **b** an air core.

of curvature around $300\mu m$ and separation about $100\mu m$ the coupling efficiency $\varepsilon = [2\omega_f\omega_m/(\omega_f^2 + \omega_m^2)]^2$ could reach 80%[3], and you can find the definition in 1.6.3. But when the radius of curvature reduced to about $10\mu m$ in the cQED system, the coupling efficiency reduced to $\varepsilon \approx 23\%$ [9]. For the trap we are to install, the cavity distance is around $400\mu m$ and the radius of curvature is about $250\mu m$. So, we would still expect a good coupling efficiency, while requiring a lot of work for the mode matching.

By implementing the substrate micro-cavity method we could overcome the disadvantages when using fiber-cavity of mode-matching and polarization problems. The cavity shall be accessed by free beam coupling which allows good mode-matching and offers full polarization control in excitation and detection[5] which could possibly results in better performance than fiber-based cavities. And as the substrates we plan to use are also based on silica, similar fabrication used to produce fiber tip mirrors could be implemented to the substrate cavity manufacturing and similar parameter space configuration is expected.

1.5 Polishing pulse

Sometimes when the cleaving surface of the fiber is not good enough or there is roughness on the substrate, we apply a polishing pulse to reduce the roughness of the target area. The method is to apply pulses of low power and long duration to melt the surface a little in order to flatten it. Because only a thin surface is melt, the overall geometry of the concave profile is not changed, while the roughness is reduced. Though it is meant to only melt the surface without induce ablation effect, we could still observe ablated particles at the periphery of the polishing area under the AFM. It's

not expected but the density is low. This phenomenon is also observed in other experiments like [6].

1.6 Cavity and coupling parameters

Most of the contents of this section is from these text books[12, 21] and Hunger's paper[9] published in 2010 which I found very useful.

1.6.1 Definition and optical parameters

We shall first label the two mirrors of the cavity as $i = 1, 2$, with corresponding mirror parameters of radius of curvatures (ROC) R_i , diameters D_i , intensity transmission \mathcal{T}_i , scatter and absorption losses $\mathcal{L}_i = \mathcal{S}_i + \mathcal{A}_i$, and reflectivity $\mathcal{R}_i = 1 - (\mathcal{T}_i + \mathcal{L}_i)$. Basic parameters associating the cavity are the optical distance L between the mirrors, the round-trip loss $\mathcal{L}_{tot} = \mathcal{T}_1 + \mathcal{T}_2 + \mathcal{L}_1 + \mathcal{L}_2$ neglecting clipping loss, the free spectral range $FSR = 2\pi c / (2L)$ in vacuum and the full-width at half-maximum (FWHM) frequency $\delta\nu$ or expressed as the half-width at half-maximum (HWHM) angular frequency

$$\kappa = \frac{2\pi\delta\nu}{2} = \frac{c\mathcal{L}_{tot}}{4L} = \frac{\pi c}{2L\mathcal{F}}$$

which is frequently used in CQED, the quality factor $Q = \nu / \delta\nu = \mathcal{F}L / (\lambda/2)$, and the cavity finesse

$$\mathcal{F} = \frac{FSR}{2\kappa} = \frac{FSR}{2\pi\delta\nu} = \frac{2\pi}{\mathcal{L}_{tot}}$$

which only depends on the properties of the mirror surface coatings and is not related to the cavity length.

1.6.2 Waist radius

To reach a strong coupling between the light and the matter, a small beam waist at the interaction spot is required. Usually the smaller the waist radius, the bigger the intensity. In the symmetric case for the radius of curvatures, which is similar to ours, $R_1 = R_2 = R$, the waist radius expression could be reduced to

$$\omega_0 = \sqrt{\frac{\lambda}{2n\pi}} (L(2R - L))^{1/4}$$

which is much simpler than the full expression

$$\omega_0 = \sqrt{\frac{\lambda}{n\pi}} \left(\frac{L(R_1 - L)(R_2 - L)(R_1 + R_2 - L)}{(R_1 + R_2 - 2L)^2} \right)^{1/4}$$

[21]. For macroscopic supermirrors, the region $\omega_0 \leq 5\mu m$ that causes interest in many cavity systems is only possible in the near-concentric regime

$L \sim 2R$, which is so difficult or nearly impossible due to the extreme sensitivity of the alignment[9] as it's close to the stability limit. It is said that the existing macroscopic FP cavities normally have $\omega \sim 20\mu m$. In our case $R \approx 300\mu m$, which is two to three orders smaller than a macroscopic one. And with a cavity length in similar order we would expect significant reduction of waist radius for micro-cavities. For the wavelength of $854nm$ and a cavity length around $400\mu m$ with $R \approx 300\mu m$, a waist radius of $6\mu m$ is easily achieved, and it's even far from the concentric stable limit. In our case when the cavity distance is too short, it could disturb the trapping potential and cause heating[3] so the cavity length is expected to be around $400\mu m$ and the corresponding ROC is expected to be between $250 \sim 300\mu m$ to make the cavity stable while having a desired small waist radius.

1.6.3 Fiber coupling

The coupling efficiency we are to discuss affect how good we could detect the photon emitted by the ion. We are not going to discuss the coupling between the input laser and the cavity because no known literature thoroughly discuss it. Some guys calculated the input coupling efficiency based on mode matching model[2], but only different EM modes are considered. The size matching problems for the same mode is still to be explored. A complete expression for the coupling efficiency neglecting misalignment between the mirror and the output fiber axis is[9]

$$\varepsilon = \frac{4}{\left(\frac{\omega_f}{\omega_m} + \frac{\omega_m}{\omega_f}\right)^2 + \left(\frac{\pi n_f \omega_f \omega_m}{\lambda R}\right)^2}$$

where ω_f is the radius of the Gaussian transverse mode profile for the SM fiber, ω_m the radius of the cavity mode at the fiber surface, n_f the refractive index of the fiber core and R the radius of curvature of the mirror. As typical wavelength we are using is around $854nm$. You can see a plot of the coupling efficiency with a fixed $\omega_f = 10.2\mu m$ in figure 1.3

As we are using symmetric cavity, we could derive the simple expression for

$$\omega_m = \omega_0 \left[1 + \left(\frac{\lambda L}{2n\pi\omega_0^2} \right)^2 \right]^{1/2} = \sqrt{\frac{\lambda}{\pi}} \left(\frac{LR^2}{2R - L} \right)^{1/4}$$

, which you could see a contour plot in figure 1.4. Because the fiber we are using has the fiber mode radius of $10.2\mu m$, we pick $L = 350\mu m$ and $R = 250\mu m$ as the desired parameters.

The second term at the denominator is caused by the lensing effect. When the fiber is nearly matched, $\omega_f \approx \omega_m \approx 10\mu m$, the lensing effect term is still big around 4. So, we would expect the optimized coupling efficiency to be around 50% in our case. As you can see on the plot, we still could achieve great coupling efficiency if we have a larger radius of curvature, but that

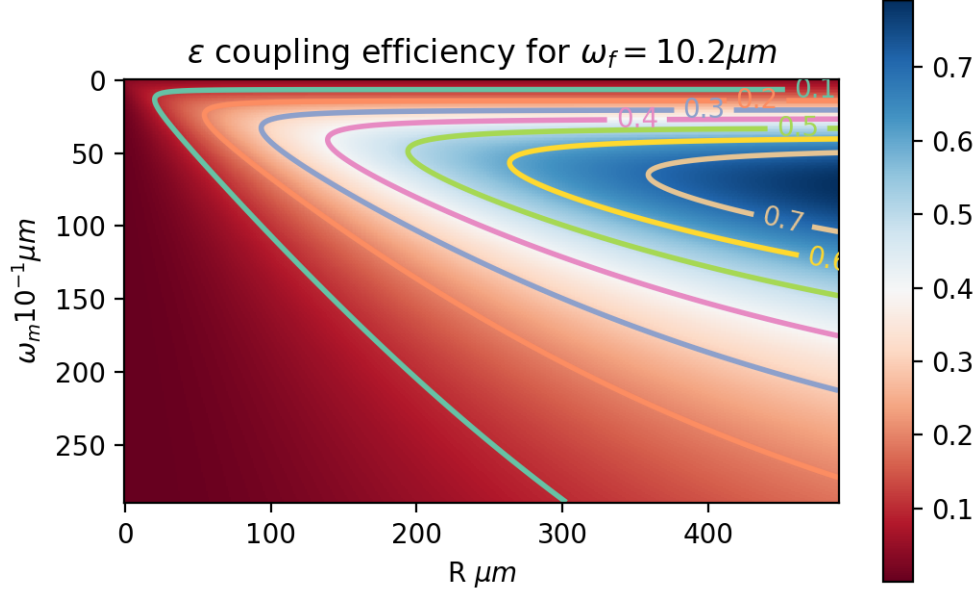


Figure 1.3: Contour plot of the coupling efficiency with $\omega_f = 10.2\mu m$

would also make the waist radius bigger and thus reduce the intensity at the center.

As for the clipping loss for a single reflection,

$$\mathcal{L}_{cl} = \exp(-2(D/2)^2/\omega_m^2)$$

, where D is the diameter of the fiber. we simply try to put a limit of 10% to the total loss to it,

$$\mathcal{L}_{cl} < 0.1\mathcal{L}_{tot} = \frac{\pi}{5\mathcal{F}}$$

leading to

$$\omega_m < \sqrt{\frac{D^2}{2 \ln \frac{5\mathcal{F}}{\pi}}}$$

. The diameter of the mirror we are creating is about $160\mu m$, and the finesse is theoretically 10^5 . So the cavity field mode radius should be less than $16.345\mu m$. Even when we set the ratio of the total loss to be 1%, the maximum cavity field mode radius is still bigger than $14\mu m$, so the clipping loss here actually wouldn't affect our experiment much under our setup parameters.

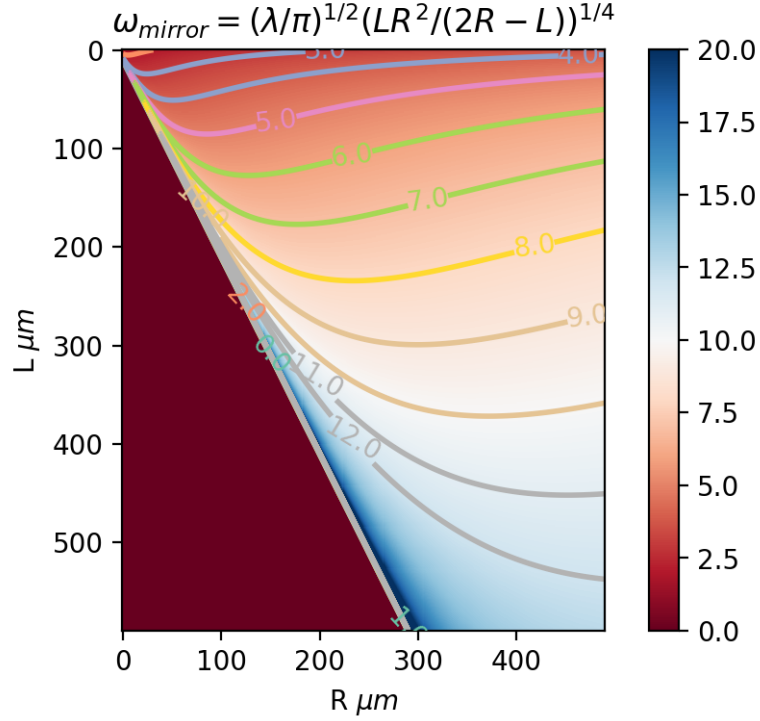


Figure 1.4: Contour plot of the cavity mode radius

1.7 Ablation process

We can construct the model discussed in [8] by treating the surface to be infinitely large. The laser pulse is treated as a square wave function so the intensity is taken to be constant over the duration. The beam profile is Gaussian $I(r) = I_0 \exp(-2r^2/\omega^2)$ and the surface local temperature is calculated only by considering the absorption of the laser beam. Also the absorption coefficient A , thermal conductivity κ and thermal diffusivity D of the fiber material is considered. Thus, we are able to obtain the surface temperature profile as

$$T(r, \tau) = \frac{A\omega^2 I_0}{2\sqrt{\pi}} \frac{\sqrt{D}}{\kappa} \int_0^\tau \frac{e^{-\frac{r^2}{\omega^2/2+4D\tau'}}}{\sqrt{\tau'}(\omega^2/2+4D\tau')} d\tau'.$$

The temperature at the center could be calculated analytically as $T(0, \tau) = AI_0\omega/(\sqrt{2\pi}\kappa) \arctan \sqrt{\tau/(\omega^2/8D)}$. And the corresponding ablation rate can be roughly written as

$$v(r, \tau) = v_0 e^{-U/(k_B T(r, \tau))}$$

1. INTRODUCTION

where U should be the latent heat of removing an atom. To calculate the radius of curvature of the ablated profile, we shall integrate $depth \sim \int_0^\tau v(0, \tau') d\tau' \sim \tau e^{-b\tau^{-1/2}}$ so that $ROC \sim depth^{-1} \sim \tau^{-1} e^{b\tau^{-1/2}}$. Later in section 2.4.1 we use this function to fit our experiment data and is good as expected.

Chapter 2

Fabrication

We start the fabrication of FFPC using the setup borrowed from Atac Imamoglu's group. We first tried the single shot laser ablation based on their setup. After probing through the parameter space, we are able to obtain nice concave profile on the tip of the fiber. Then we installed a rotational fiber holder to implement the multi-shot laser ablation to further reduce the asymmetry. Later to speed up the production, we further integrated the setup with motorized stage to completely automatize the fabrication process with a LabVIEW program and Python scripts. And at last we implement the substrate ablation and polishing test.

2.1 Optical setup

You can see our setup for fiber tip ablation in figure 2.1, and the modified setup for substrate ablation in figure 2.2. The difference is that we moved the substrate backward for some distance because the substrate might touch the imaging system if we directly replace the fiber stage with the substrate one. So we add another lens to move the focusing point 4cm back.

Actually all the parts which have possibility of direct contact with the CO₂ laser beam are contained in a big box with glass windows and doors on each side. It is designed so because if the CO₂ laser beam is scattered, it won't get out of the box for silica can absorb the scattered light with that wavelength.

We can divide the whole setup into 3 parts. First, there is a CO₂ lasing part to focus the CO₂ laser onto the fiber tip or the substrate. The laser we are using is Firestar OEM v30 and the output wavelength is 10.2 μ m. We could also tune the output lasing intensity by rotating one of the Brewster polarizer. There is also a wave plate at the end to change it to circular polarization to make the ablated profile less elliptical. For triggering the CO₂ laser, we use an Arduino UNO to sent signals to trigger the pulse and control the pulse duration.

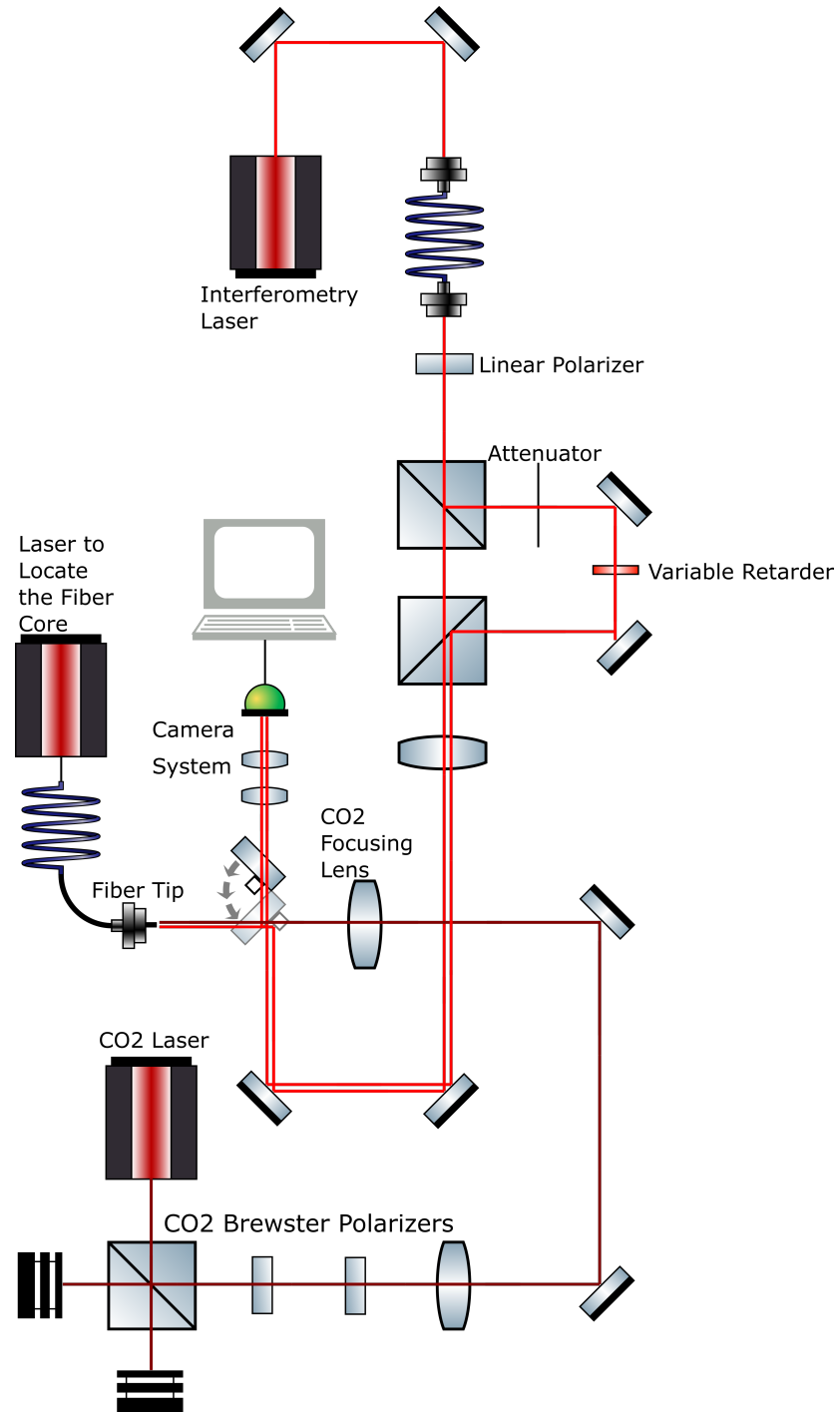


Figure 2.1: The setup for fiber tip ablation

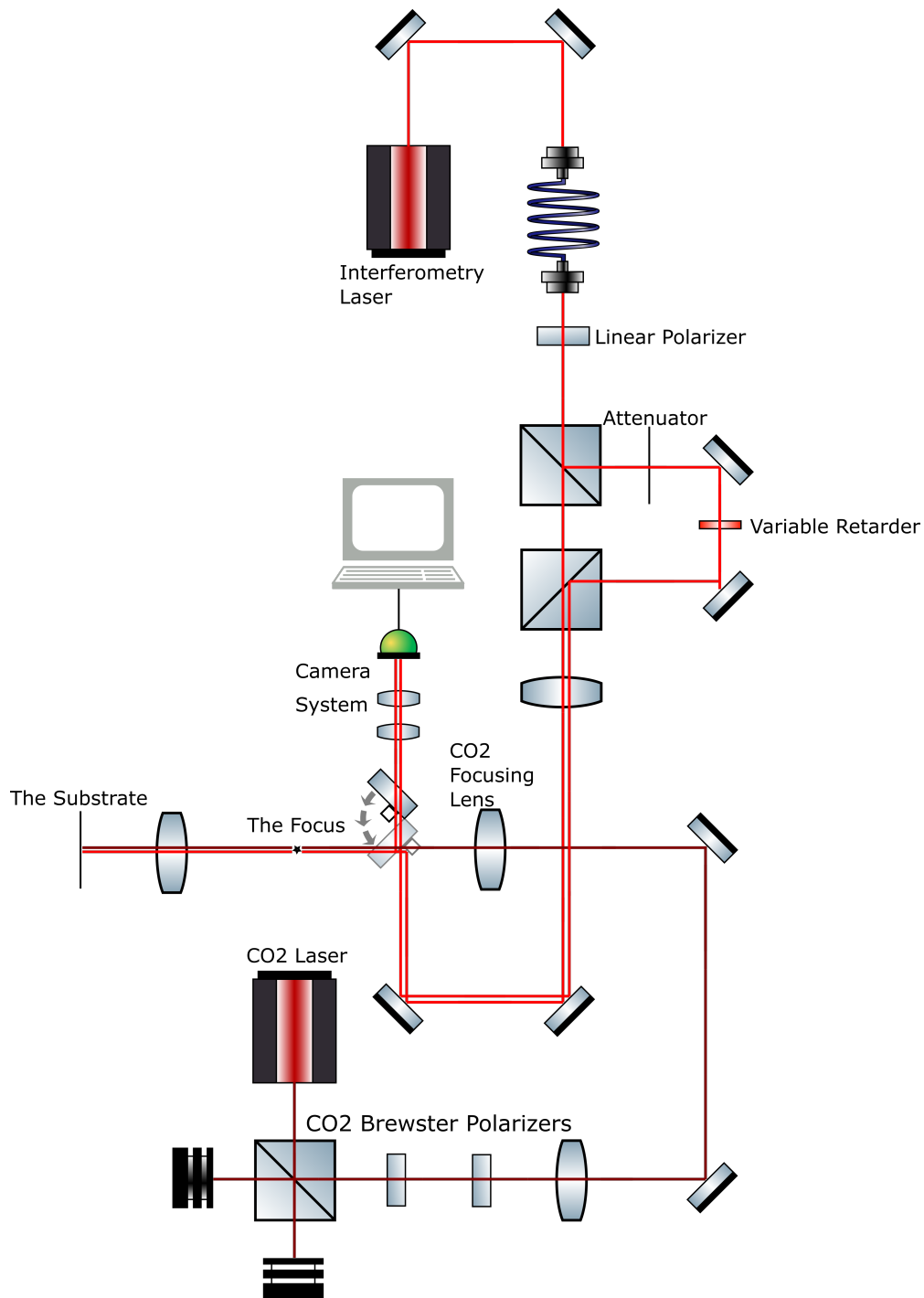


Figure 2.2: The setup for substrate ablation

The second part is for the interferometry imaging. Currently we are using a 623nm laser to form interferometry pattern on the image we took of the sample surface. Then we use the camera system to capture the surface pattern and use a Python script to extract the correct surface profile. There is a flippable glass plate in front of the CO₂ focusing lens. When we do the ablation, we keep it up to avoid the disturbance of the CO₂ laser. When we do the imaging, we put down the flippable glass plate so that one of the interferometry light is reflected to the surface we are to examine, and then reflected back to the glass plate and meet with the other interferometry light to form interferometry pattern. The camera system we use is capable of adjusting the relative distance from the imaging depth to the CO₂ focusing point. So we can still get a nice and clear image of the surface even if the sample is still at some distance from the CO₂ focusing point, allowing us to tune the mode radius of the CO₂ laser on the sample surface to create concave profile with different diameters. Because the other interferometry light directly goes into the camera, which is too strong for the reflected interferometry light, we put an attenuator in the light path to reduce the intensity to make the interferometry pattern clearer. We also need a variable retarder in one of the light path to tune the phase of the light in order to get different interferometry patterns with different phases which is needed in the surface extraction.

The third part is to hold the sample and adjust the position of it. We use different holders for different stages of the experiment. We eventually upgraded this part by installing three motorized stepping screws on the translation stage and a motorized precision rotation mount to do the rotation of the sample. We use a laptop to control the variable retarder, and a LabVIEW program to control the motorized stage, the camera system, and the Arduino.

2.2 Fiber preparation

For the fiber cavity we are to use PCF (photonic crystal fiber[17]). But at the starting point we use a cheaper and more flexible one with 125 μm diameter and a 10 μm radius core. We don't have a proper cleaver for this type of fiber, so multiple attempts shall be made to get a workable surface. If the tip is not nicely cleaved, there will be many tiny holes on the surface or even big structures that could cause big problems to the ablation.

2.2.1 Collapsing

For the PCF preparation, we use LMA-25 which you could see a similar cross section in figure 2.3. We do it by first collapse it using a splicer, then cleave the collapsed region. If we did not collapse the fiber before cleav-

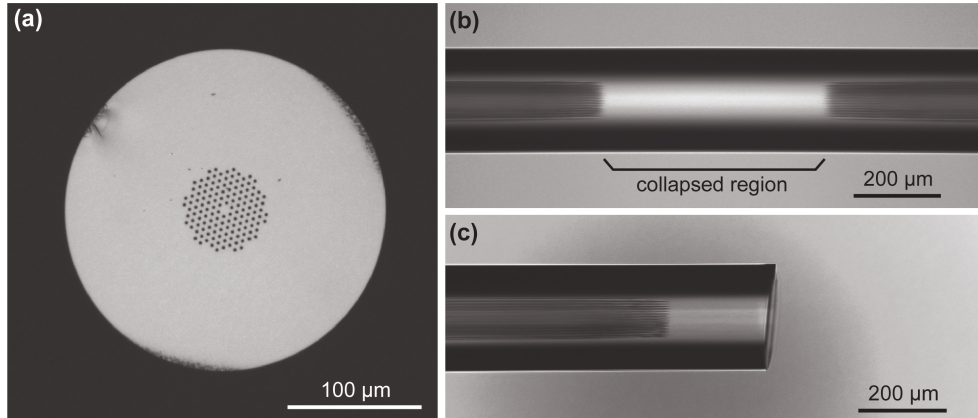


Figure 2.3: The image of a solid-core PCF[4]. **a** shows a cross section image of the uncollapsed LMA-8-UV fiber. It looks qualitatively the same with our LMA-25, it's just the difference between the core sizes. **b** shows a region of about $600\mu\text{m}$ long collapsed using a fusion splicer. **c** shows a cleaved section with a certain angle.



Figure 2.4: Collapsed tip surface of LMA-25 using our novel collapsing method.

ing, the facet is extremely hard to clean since some debris on the facet can collect in the holes and affect the coupling efficiency[4]. We try to keep the remaining collapsed region in the fiber as short as possible, because it may introduce additional expansion of cavity mode field radius before entering the core area of the PCF. We calculated this expansion and plot it in figure 2.5. It does not seem to be a great diffraction because the wave is nearly perpendicular to the curved surface so the diffraction effect is not significant. Actually, there is a difference with and without the collapsed region of about $0.11\mu m$ at the position $100\mu m$ within the collapsed region. So an easy way is to treat it as an additional cavity length before entering the core area of the PCF since the difference is so little.

Actually if you see in figure 2.6 you can compare the effect of this expansion of the field mode radius to the coupling efficiency. You will find the calculation of the mode radius in the appendix A.1.1. Even at a depth of $100\mu m$ which is already pretty small, the coupling efficiency still decreased significantly. You can find the corresponding calculation of the coupling efficiency in the appendix A.1.2. This is one big problem to be resolved in the future. Recently effort has been made to try the fiber integrated mode matching between the input/output fibers modes and the cavity mode[7]. In this case the mode from the cavity to the fiber is remodulated by a GRIN fiber to match the mode. It's a great work but it's too hard for us to implement the GRIN method to integrate the fiber tip with this technology. But it is also shown that the fiber length can be accurately controlled by cleaving method mentioned in [20]. It is stated that under the microscope, the accuracy of the cleaving can be constrained within $15\mu m$. With a collapsed region with about $15\mu m$ is relatively acceptable for us.

Another way to control the collapsed region depth is to first cleave the fiber, and then use the splicer to collapse it. You can see one sample tip surface in figure 2.4. This is a much easier and reliable approach. The splicing parameters we need to tune are the gap, current and its duration. We perform a rough optimization over the parameter space until we get a surface with very thin collapsed region less than $10\mu m$ and still reasonably flat. We examine the depth using a microscope by first focusing onto the tip surface, then focusing onto the air holes and measure the distance between these two interfaces. Our ablation depth is well below $10\mu m$, as long as we are using multi-shot approach which only apply moderate modification to the surface each time, we won't worry about the cavity shape deformation caused by the air holes inside the PCF. But there is one big problem for this method which is that you can not really get a nice flat surface. And since the ablation would usually induce a certain depth of collapsed region about $20\mu m$, using the normal way to cleave the fiber is just fine because under the microscope we are able to restrict the collapsed region after the cleaving within $20\mu m$ and it already satisfies our need.

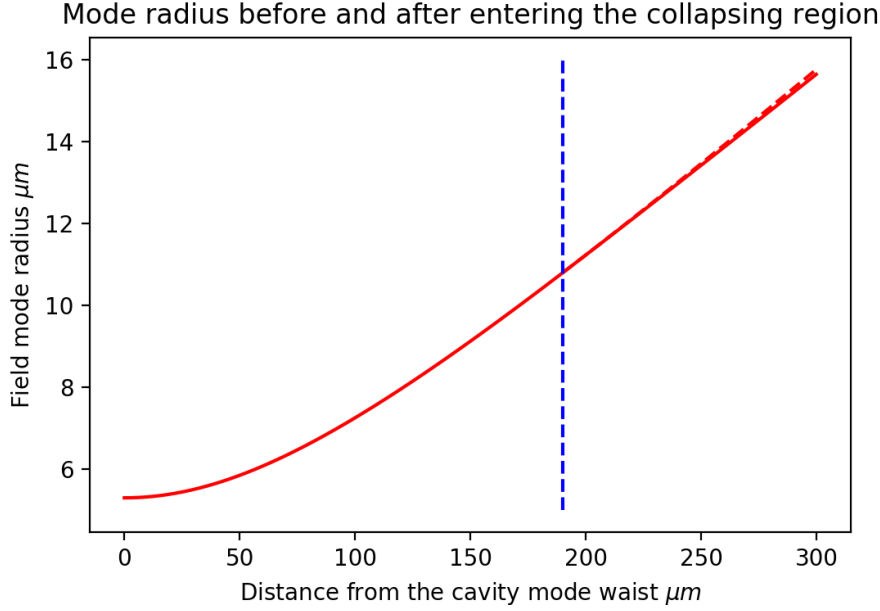


Figure 2.5: Mode radius calculated from the waist of the cavity to $100\mu m$ within the collapsing region. The red dashed line on the right is the radius without the fiber.

2.2.2 Splicing

As PCF is really fragile, it is not recommended to conduct the whole manufacturing using a long PCF fiber. What we do is to first cut a reasonably short piece of PCF, conduct the whole manufacturing procedure, and splice it with a longer PCF to reach the length we need. Usually commercial splicers have predefined programs to splice conventional fibers together and are really robust. In our case we need to explore the right splicing parameters our own since no splicer has a predefined program for PCF fibers. You can find a document[15] here providing some basic suggestions for the PCF splicing, but no parameters are given for LMA-25.

Thus, an optimization must be performed to get the splicing working. We start from a program defined for LMA-10 modified by one of our group member before. The splicer first space the fiber tips by the distance defined by GAP, then conduct the current sequence $CURRENT_i$ and $DURATION_i$ to heat them up while slowly move the tips closer to each other. At last the tips are pushed together by the distance defined by OVERLAP. The current sequence have three currents to define. We use the first current as a prewheating for the fibers, then the second current as the parameters to optimize and the third current as a relaxing current. Thus, we choose GAP, OVERLAP, $CURRENT_2$ and $DURATION_2$ as the four main parameters to

2. FABRICATION

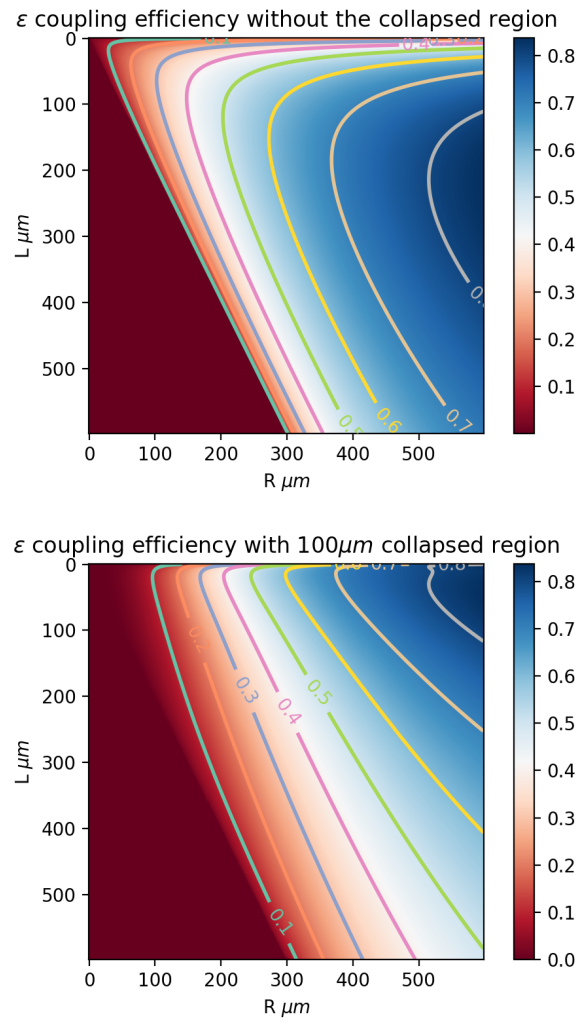


Figure 2.6: Coupling efficiency calculated with and without the collapsed region

Table 2.1: Parameter settings to optimize applying Taguchi L9 orthogonal array method

Experiments	Parameters to optimize			
	GAP	OVERLAP	CURRENT	DURATION
1	1	1	1	1
2	1	2	2	2
3	1	3	3	3
4	2	1	2	3
5	2	2	3	1
6	2	3	1	2
7	3	1	3	2
8	3	2	1	3
9	3	3	2	1

optimize for the LMA-25 splicing.

One big problem for the parameter optimization is that the preparation of the PCF fibers before the splicing takes lots of time and they are really expensive. So it is not realistic to explore the whole parameter space. We first try three candidate values for each parameter that are reasonably near the one that is workable for the splicing. If we try all the combination, it will be $3^4 = 81$ parameter settings to explore, not to mention the repetition of each parameter setting since the outcome might differ a lot each time for some settings. Thus, we use the Taguchi L9 orthogonal array which you can see in table 2.1 to reduce the number of the settings we are to try. The numbers 1, 2, 3 in the column indicates the three reasonable values we choose for each parameter. Using this experiment design, we only need to determine how these nine settings perform to get a rough idea about around which setting we might get a fully optimized performance.

But for each trial we make, the loss is also affected by many factors. The mostly influential factor is the cleaving. The cleaved surface sometimes has a certain angle which will induce angular misalignment for the fibers. In this document[15] you can see that for the $15\mu m$ mode field fibers, even an angular misalignment about 1.0° could induce about $1.5dB$ splice loss in the fibers. So we try several times for each setting and choose the best result we got.

The PCF fiber model LMA-25 has a skyrocketing attenuation of light under the wavelength of $850nm$ as you see in figure 2.7. So, when measuring the splicing loss, it is not recommended to use a normal laser pen which usually has the wavelength around $600nm$ as the power input. We used $780nm$ laser and the attenuation is measured to be $0.730dB/cm$ as you can see in figure 2.8. Because our cavity is aiming for $854nm$ wavelength, it is not recommended to use this type of PCF if you are planning to use any wavelength

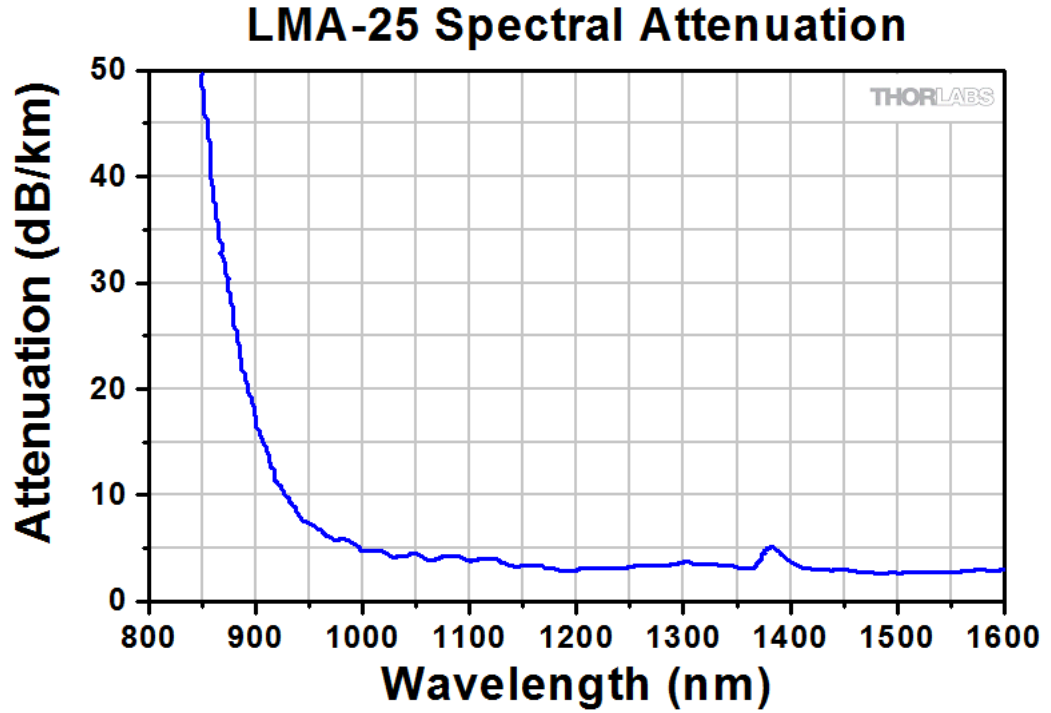


Figure 2.7: Spectral attenuation of LMA-25 from Thorlabs website.

under 850nm . If you are planning to use wavelength above 500nm and under 850nm , LMA-20 is recommended but it will also decrease the coupling efficiency by a considerable amount.

Before I went back to China I don't get enough time to measure all the parameters using the right wavelength. It's time consuming and our splicer don't have a facet view so we don't really know if the air holes are aligned as well. But during our tests we found some parameter regime might be worth exploring: the GAP between $50\mu\text{m}$ – $80\mu\text{m}$, OVERLAP between $8\mu\text{m}$ – $15\mu\text{m}$, Current 1 of 10.5mA with 1.5s , Current 2 of 10.5mA with 2.5s (or 12.5mA with 1.5s) and Current 3 of 7.0mA with 0.5s .

2.2.3 Ablation simulation

In order to get a better understanding of how the ablation works and what time region we are to work with, we did a Comsol simulation of the ablation process to see how the heat propagates and how precisely we need to control the pulse duration to get a desired curvature.

You can see one of our simulation results in figure 2.9. The ablation model we use is from [13], which estimate the ablation threshold temperature to be around 3085K . We define a heat flux with a Gaussian power distribution and a beam radius of about $100\mu\text{m}$. The resulting ablation depth for pulse

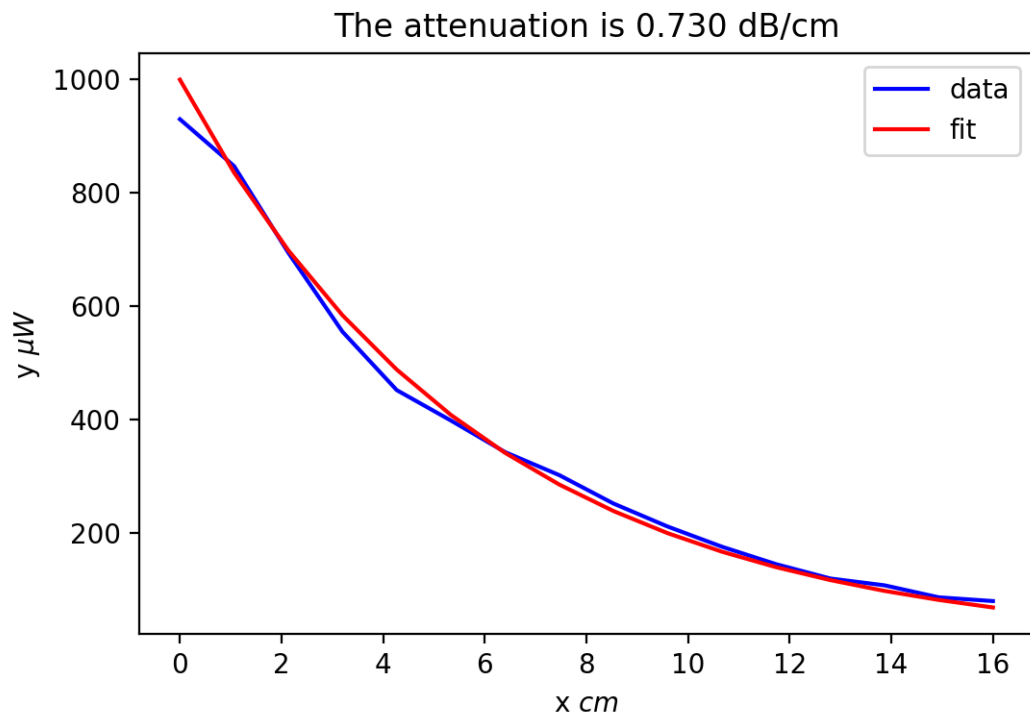


Figure 2.8: Measured LMA-25 attenuation at 780nm.

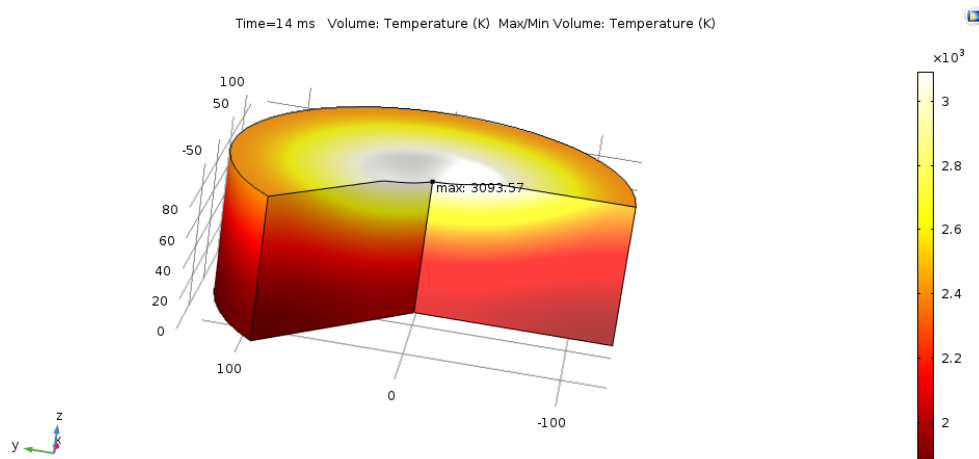


Figure 2.9: One of our simulation results using COMSOL Multiphysics.

duration between $12ms$ and $14ms$ is still modest, but for longer duration the concave hole is just too deep and too big for the mirror in our case. This behavior of short workable duration range is also observed in the experiment. The soften point for fused silica is around $1900K$, so the thin region near the tip surface is softened, and the surface is believed to be melted. Though the concave hole does not cover the whole surface, considering the fiber field mode radius is only $10.2\mu m$ and the cavity field mode radius is no more than $12\mu m$, it should be large enough for the cavity.

We can also get a feeling about what time regime would the polishing parameters be in using the simulation. But since the experiment is more complicated a situation, it makes more sense to determine the parameters experimentally. But the relation between the pulsing time and the ablation depth meets what we derived in section 1.7.

2.3 Ablation procedure

For the fibers, we first fix it onto the holder and shine a laser which you can see in figure 2.1 through the fiber so we could make it easier to find the fiber position and move it to the camera sight.

We control the CO_2 laser using an Arduino UNO. When we first initialize the Arduino board, the output port might has a voltage vibration and is not safe if the lasing control button is on on the output side. So, please make sure that you first initialize the Arduino, then turn the control button on and proceed.

For marking the position of the CO_2 laser focus, we first use a white paper to block the lasing path and with moderate pulses we can get a black point on the paper, indicating the rough position of the focus. Then use a fiber to do testing shots until we see that the fiber gets ablated which means that we could truly locate the focus of the CO_2 laser. Once the position of the focus of the laser is determined, we mark a digital point on the camera screen to indicate the focus point. After we determine the position of the focus point, we still need to update its position each day because it could slightly change due to the position shift of some optical components due to daily operations, but normally it won't change more than $30\mu m$ if the setup is not heavily disturbed.

Though the position on the camera screen is determined, it still has a value in another axis undetermined, which I shall call it the depth because it's vertical to the camera screen. We could mark this position by adjusting the camera imaging point where the tip becomes clear. By comparing the diameter of the hole ablated on the fiber tip with different imaging depth, we are able to get one certain depth corresponding to the minimal diameter of the ablated hole. So each time when we adjust the image depth to this value and adjust the position of the fiber tip to make the tip image clear, we know

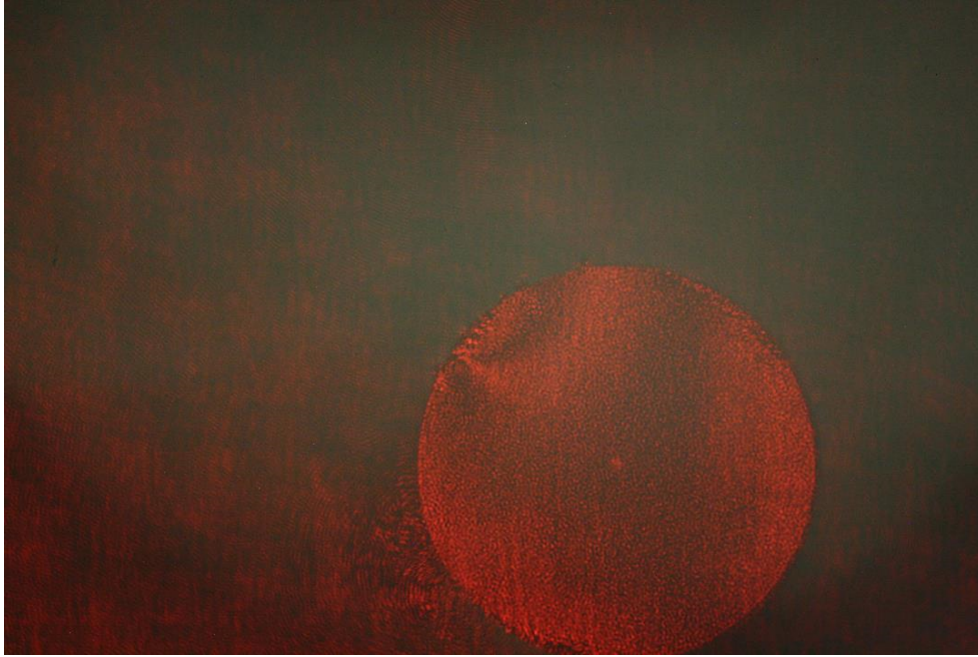


Figure 2.10: A nicely cleaved fiber surface perpendicular to the interferometry light

that the fiber tip is at the right depth where the CO_2 laser focus is. In our trial experiment, we could get a minimal diameter of ablated holes down to $10\mu\text{m}$. But as we are aiming for a concave mirror with diameter around $90\mu\text{m}$, we actually change the depth of the image point a little bit deviated to expand the interaction area on the fiber tip.

Then, we still need to tilt the fiber surface direction because if it is not perpendicular to the interferometry laser, there will be massive patterns in one direction impeding surface analysis. If the surface is nicely tilted and it is perpendicular to the interferometry light, you are expected to see only a very small number of patterns on the surface, like the one shown in figure 2.10.

After the alignment, we are able to test pulses with different power and duration to get concave structure with different diameters and radius of curvatures. We can't directly read out the power from the markers on the Brewster polarizers. So we used a PD to get the value of the power at the interacting area corresponding to certain readings from the polarizer. We then use the surface analysis to extract the surface profile, and determine which pulsing parameter is the desired one.

When applying the multi-shot laser machining method, we need to rotate the fiber after certain number of pulses. To ensure that the fiber position does not move significantly after gets rotated by a relatively small angle, we

use a homemade rotational holder to fix the fiber tip near the rotational axis. We try to keep the fiber tip still on the camera screen after a relatively small rotating, automatically analyze the position and move it back to the focus. Thus, we are able to rotate the fiber to any angle we want. Right now with our homemade fiber holder designed by Klara, we are able to maintain the fiber position within the camera range within a full round rotating. But the motorized rotation holder also has the heavy weight problem for us. After we installed the holder onto the translation stage, we observed significantly increased tiny vibrations of the objects on the camera screen. The vibration is about $1\mu m$ magnitude and is causing the interferometry pattern vibrating, which is a big problem for the surface profile extraction if we can't get nice and stable interferometry pattern. We suspect that it's the heavy weight of the holder with the unstable structure of the mirror tilting holder that's been holding the fiber holder is causing this vibration. So we use "Blu Tack" which is a commercial soft solid stick to stick onto the connections of the setup, trying to reduce the vibration. There is no significant change on the camera screen, but when you use the camera to take a shot, the interferometry pattern on the screen is much more clear than before. And after we move the setup to a much isolated position, the vibration reduced greatly so the surface analysis is working again.

The fabrication sequence is controlled by a LabVIEW program written by me. If we do not know the position of the CO₂ laser focus, we should first take test shots and move the fiber core to the focus position. Then we use the program to calculate the position of the focus. This could be a daily procedure to update the position of the focus. For the ablation sequence, We first move the fiber into our sight in the camera screen and turn on the locating laser connected to the fiber, the program controls the camera to take a shot, uses a Python script to identify the position and calculate the relative distance to the CO₂ laser focus point, controls the translation stage to move the fiber to the focus point, controls the rotation holder to rotate a relatively small angle (like 45°), takes a shot, analyze the relative move and record it, move the fiber back to the focus, repeat several times until a 90 degrees rotation is completed. In this way we get records of how we should move the fiber after each rotation. Then we start from the beginning, apply several pulses, rotate and move the recorded relative distance, continue the same sequence described above until a full round is completed. The sequence described above is could be automatically done by the LabVIEW program. The core part of this program written by me is aligning the fiber to the CO₂ laser focus position. So you can use whatever method that suits you to complete the sequence described above. You will find the instruction for this program in the Appendix A.2. The Python scripts the LabVIEW program calls for analyzing the position of the fiber can be found in the appendix as A.3.2 To determine the position of the core (normal fibers), A.3.4 To determine the size of the field beam (normal fibers) and A.3.3 To determine the position of

the core (PCF fibers).

2.4 Surface analysis

We use the interferometry image to get the surface profile. It is a quick approach to get most of the parameters of the surface structure like the ROC of the concave profile. But due to the resolution problem, we further use a AFM to examine the fiber tip to get a far better resolution of the surface roughness.

2.4.1 Interferometric surface analysis

We use the images captured from the camera to further extract the surface profile using a Python script. PIL package is used to import the images. We directly use the intensity from the image as the light intensity, ignoring the gamma setting when the image is captured. We use four images with different pattern phases of $0, \pi/2, \pi, 3\pi/2$, then use the following formula to extract the phase of each pixel (m,n) in $[-\pi, \pi)$,

$$\theta'(m, n) = 2 \tan^{-1} \frac{I_1(m, n) - I_3(m, n)}{I_2(m, n) - I_4(m, n)}$$

, with I_i corresponding to the intensity number of the pixel (m,n) in the i th image and is believed to have the form of $A + B \cos \theta_i$. The θ' here is actually twice of the actual phase. The reason we time 2 is because we need a θ' in the range of $[-\pi, \pi)$ to use the function `unwrap_phase()` from the package `skimage.restoration` to restore the actual phase so that we could further calculate the height for each pixel using $h = \frac{\text{unwrap_phase}(\theta')/2}{2\pi} \lambda$.

After we extract the surface profile, we use a 2D Gaussian function to fit the profile to further extract other parameters like ROC of the concave, asymmetry and data deviation from the fit. You can see one of our analyses of the tip surfaces in figure 2.12. By using the interferometry image to extract the surface profile, we can quickly determine if the sample we make has the desired parameters. After collecting enough samples produced under different pulse parameters and by different procedures, we take them under the AFM to further examine the surface roughness to see if the surface is actually smooth enough to exhibit high finesse.

You can find the major part of the Python code used to analyze the tip surface in the appendix A.3.1.

Using the interferometric surface analysis, we are able to roughly identify the radius of curvature for each pulse parameter setting we use and thus find the right parameter setting for our desired radius of curvature step by step. Eventually, we are able to achieve nice $160\mu m$ diameter concave profile

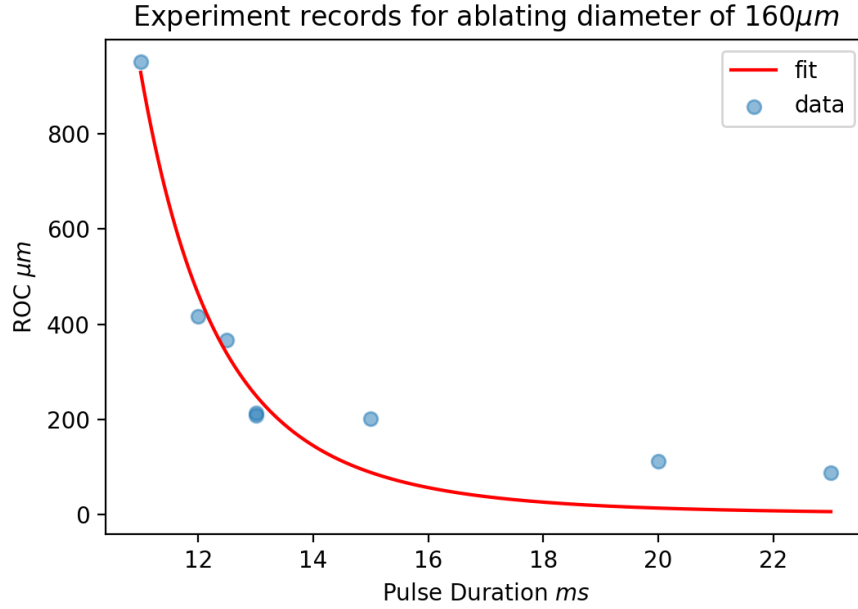


Figure 2.11: The data records for the PCF LMA-25 ablation parameter setting of: Brewster marker 25 (nearly full power output), ablating diameter $160\mu m$. We eventually choose this parameter setting considering the repeatability and the fiber size. The fitting uses an approximation of the equation derived in section 1.7 and it's good as expected.

with the radius of curvature around $350\mu m$ and the asymmetry below 5% using the PCF LMA-25. You can find one of our data records in figure 2.11. We use an approximation of the equation derived in section 1.7 to fit the result and the fitting is good as expected. The retardance setting I use for our interferometry laser is $100nm, 259nm, 418nm, 577nm$, well within the linear regime.

2.4.2 AFM surface analysis

We use the AFM in the cleaning room to further examine the surface roughness of the concave structure on the fiber tip. Because the fiber we are to coat is extremely fragile, we are not able bend it to keep the whole fiber to fit in the AFM. Thus, we cut the top $1cm$ tip to glue it on a sample holder using the First Contact for the AFM examination. After that the samples we made are not long enough for the cavity anymore, so this procedure is mainly to determine if the pulse parameters are good enough to produce smooth surface. The ones that are made for coating won't go through this

2.4. Surface analysis

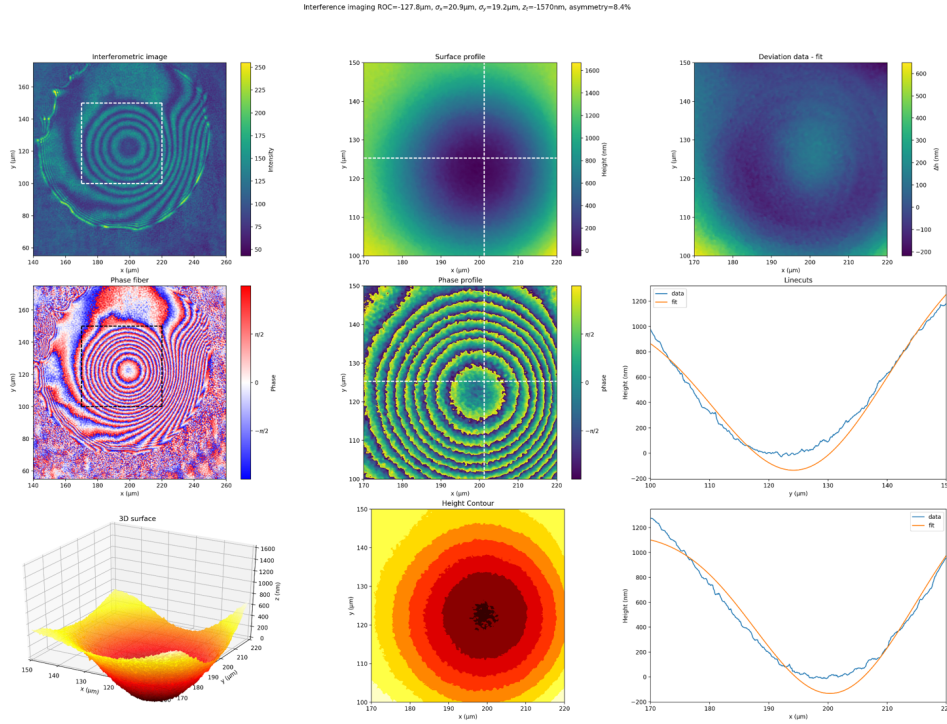


Figure 2.12: Surface analysis using our Python script

step.

You can see the scan images of two of the samples in figure 2.14. The multishot sample is ultra smooth and we estimate the surface roughness to be less than 1nm . You can see the fitted roughness in figure 2.15. We have an additional smoothing pulse applied to this sample. You might be able to see some wave-shaped stuffs in **b**. These are the stuffs that we don't believe that are actually there. They might be caused by the AFM errors. You can see a much rougher surface in **cd**. The big structure you could see is not the stuffs supposed to be there. We believe it's some stuffs that contaminate the fiber tip after the ablation. So, the fibers should be preserved really carefully. There are still some areas from **cd** can be used as a reference for the roughness of the single-shot fiber such as the upper right and the lower right part. It's really hard to compare but you can see that the single-shot fiber is still very smooth for most areas, except that for the upper right part we don't know if the particle there is a contamination or an ablated particle. If it's a contamination, we could say that single-shot fiber is not bad, but if it's a particle caused by the ablation, then a polishing pulse is really necessary to ensure a smooth surface.

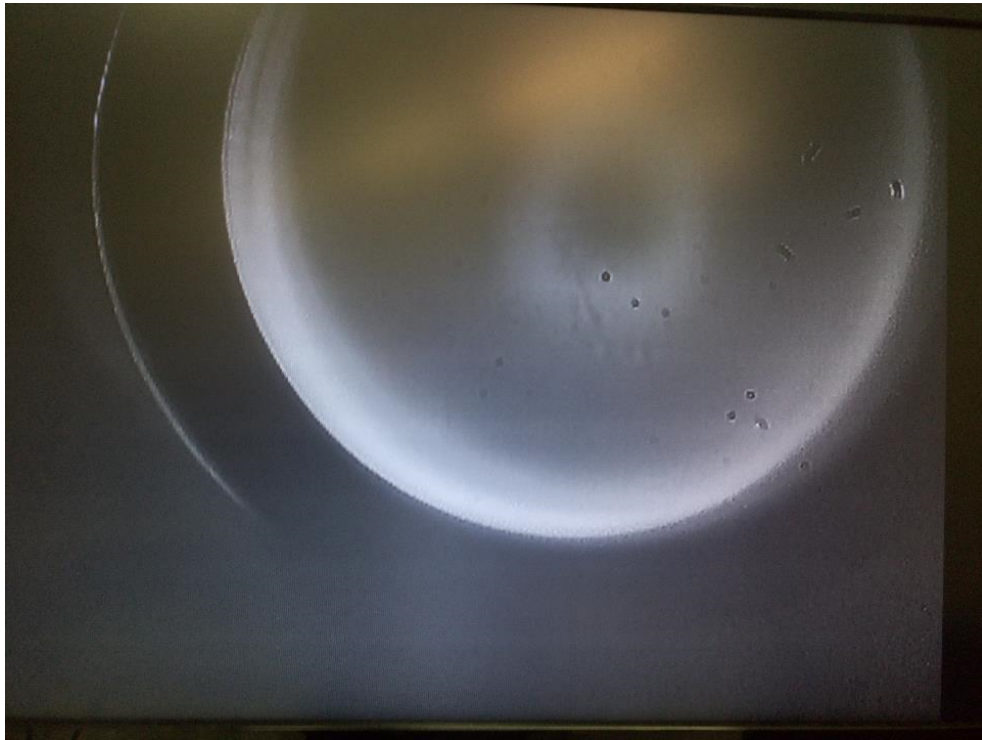


Figure 2.13: The image of an ablated LMA-25 fiber tip which collapsed first. The dust in the image is from the microscope.

2.5 Fiber coating

I don't know by the time my internship is finished if we are able to finish the fiber coating. We haven't started yet, and it seems to be a lot of problems with coatings to be overcome. As it is stated in 1.6.1, finesse is determined by the properties of the mirror surface coatings so that it's of great importance. Usually the coating would have a maximum reflection at the wavelength of $823nm$. We are planning to do the coating through one of the two companies of Laser Optik and ATFilms (Advanced Thin Films). Previously there is a group[3] already tried the coating near this wavelength. The coatings were through ATFilms and great loss was introduced. The loss could be caused by the non-uniform thickness of the coatings, and defects created while annealing under vacuum environment. If we are to go that further, the paper could be used as a valuable reference.

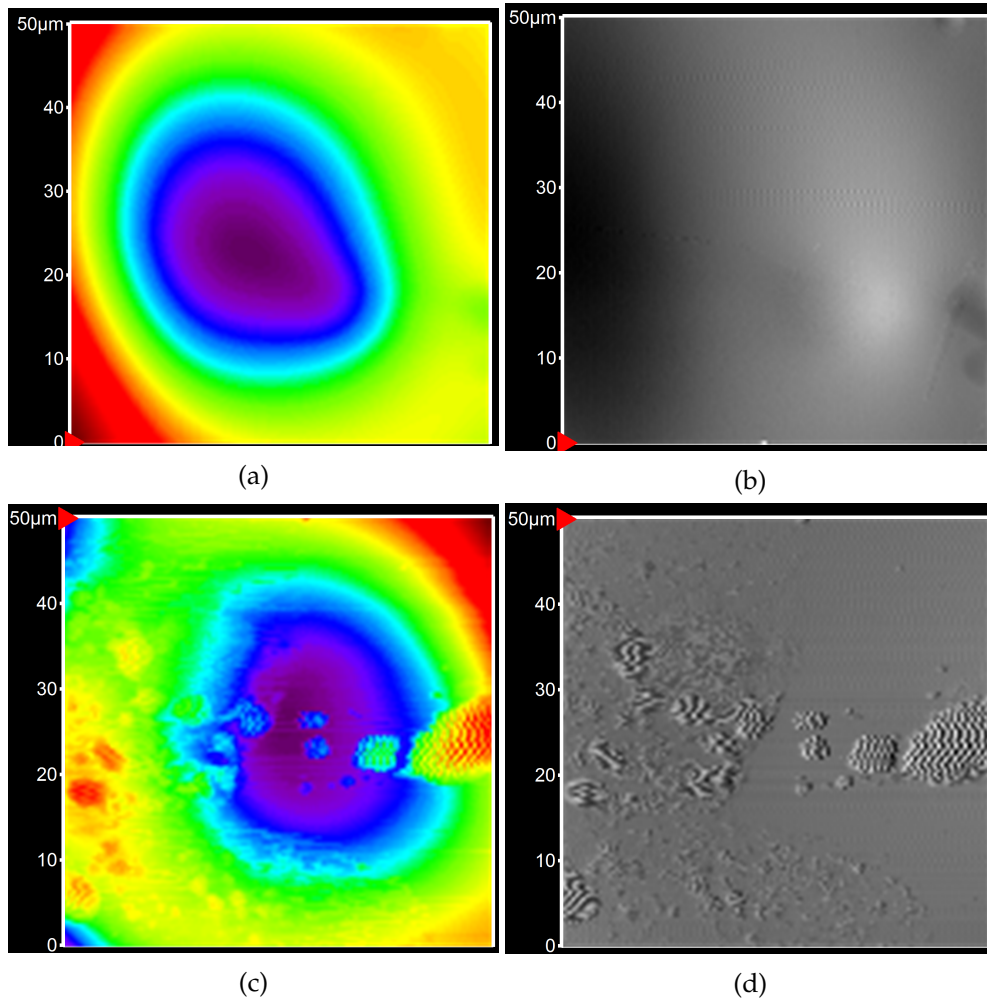


Figure 2.14: Surface check using AFM. **ab** is the height scan and the amplitude scan of a multi-shot without rotating sample. **cd** is the height scan and the amplitude scan of a single-shot sample.

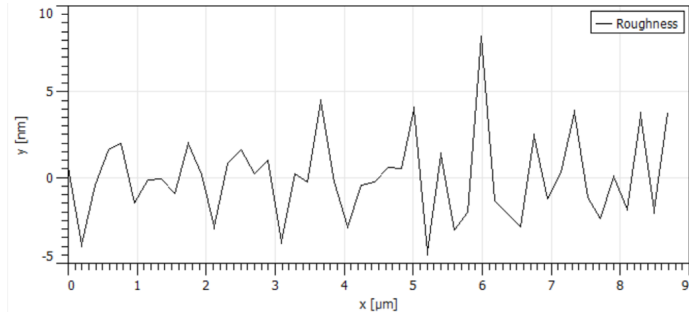


Figure 2.15: Fitted roughness using Gwyddion. We select a smooth line in figure 2.14 to fit. The oscillation is caused by the fitting because we only used the linear interpolation. Also the AFM itself created some patterns in the scanned data (which is likely an oscillation). But even if we count this kind of oscillation into our roughness, the average is still less than $2nm$. So we expect the real roughness to be less than $2nm$ which is a conservative estimation.

Chapter 3

summary

The thesis briefly discussed the research background of the optical cavities on optical fibers and substrates. It is mainly motivated by the need of the high performance ion-photon interfaces. In trapped ion systems, the miniaturised cavities are likely to be a key enabling technology to a full-scale quantum computer.

We first tried the manufacturing of FFPC with PCF which is already been explored for some years by numerous groups. We planned to do the substrate cavities which is still novel for trapped ion systems, but got no time. We also explored parameters for polishing pulse to further smooth the ablated surface. For doing the fabrication, we setup an automatic laser ablation platform controlled by LabVIEW which is compatible with both the FFPC manufacturing and the substrate cavities manufacturing. We also developed method to analyze the surface profile using interferometry lasers. For surface roughness check, we use AFM to determine and confirmed that under the parameter setting we are using the average roughness is less than $2nm$.

We calculated the desired cavity parameters in the thesis and offer solutions to some problems we have using the PCF. For the FFPC we implemented both the single-shot laser machining and the multi-shot laser machining. We first use normal fibers to explore the parameter space, and move on to PCF applying the desired parameter setting to produce mirror diameter and radius of curvature that meets the geometric configuration of the cavity integrated trap. We found that multi-shot laser machining greatly reduces the asymmetry of the concave profile, and is the most reasonable method to apply in our case. Eventually, we are able to achieve nice $160\mu m$ diameter concave profile with the radius of curvature around $350\mu m$ and the asymmetry below 5% using the PCF LMA-25.

For the substrates we were planning to implement similar procedure as the FFPC one with just a little modification of the ablation setup. Because the materials used are similar, so similar pulse parameter settings are supposed

to be working.

I don't have time to finish coating before I return to China, but the next step is to do the coating through companies and measure the cavity performance. The non-uniform thickness of the coating and defects within could introduce severe loss to the cavity, so there is still a long way to explore of this coating testing.

Ideally, we could setup a robust and fast automatic laser ablation platform of fabricating cavities on fiber tips and substrates, and high performance miniaturized cavities are fabricated that could be integrated into our cavity integrated trap.

Appendix A

Appendix

A.1 Beam propagating calculation

A.1.1 Mode radius calculation

Because the cavity is symmetric, we can determine that the waist which is at the center has a radius of

$$\omega_0 = \sqrt{\frac{\lambda}{2\pi}} (L(2R - L))^{1/4}$$

, where L is the cavity length and R is the radius of curvature of the two concave mirrors. We can then determine the complex beam parameter using

$$\frac{1}{q} = \frac{1}{R_{wave}} - i \frac{\lambda}{n\pi\omega^2}$$

, which leads to q_0 at the center to be $i \frac{n}{2} [L(2R - L)]^{1/2}$. Then any complex beam parameter in the cavity can be calculated by $q(d) = q_0 + d$. Here n should be 1, but we are to keep it. The complex beam parameter at the mirror surface is $q(L/2) = i \frac{1}{2} [L(2R - L)]^{1/2} + \frac{L}{2}$ which gives the wavefront radius $R_{wave} = R$ and the cavity mode radius

$$\omega_m(L/2) = \sqrt{\frac{\lambda}{n\pi}} \frac{(LR)^{1/2}}{[L(2R - L)]^{1/4}}$$

. This would be the one used in the expression of the coupling efficiency if there is not a collapsed region in the fiber. If we put the collapsed region into our consideration, the complex beam parameter will experience a concave lensing matrix

$$\begin{bmatrix} 1 & 0 \\ \frac{n' - n}{n'R} & \frac{n}{n'} \end{bmatrix}$$

where n is the index of the cavity and n' is the index of the collapsed region. The resulting complex beam parameter in the fiber tip is then

$$q'(L/2 + d) = \frac{q(L/2)}{\frac{n'-n}{n'R}q(L/2) + \frac{n}{n'}} + d$$

. However, since the cavity mode is always perpendicular to the mirror surface, the light is always normal incident. Therefore, we should expect $R'_{wave}(L/2) = R_{wave}(L/2)$, which is indeed the case as $\frac{1}{q'(L/2)} = \frac{1}{R} - i\frac{\lambda}{n'\pi\omega_m(L/2)}$. From here, we can derive the expression of the mode radius to be

$$\omega'_m(L/2 + d) = \sqrt{\frac{\lambda}{n\pi}} \sqrt{\frac{d^2[\frac{L}{R}(\frac{n'-n}{n'})^2 + \frac{2L}{R}(\frac{n'-n}{n'})(\frac{n}{n'}) + 2(\frac{n}{n'})^2] + 2dL + RL}{[L(2R - L)]^{1/4}}}$$

, which is already pretty much linear as you can see in figure 2.5.

A.1.2 Coupling efficiency with respect to the cavity parameters

In the previous chapter 1.3 we've already had the expression for the coupling efficiency which is

$$\varepsilon = \frac{4}{(\frac{\omega_f}{\omega_m} + \frac{\omega_m}{\omega_f})^2 + (\frac{\pi n_f \omega_f \omega_m}{\lambda R})^2}$$

. Though the expression is not valid anymore since we have this collapsed region in our PCF, we can easily replace the ω_m in the expression with the field mode radius ω'_m in the collapsed region which we've already derived in the previous subsection. The reason is that, whenever there is light emitted from the ion and transmitting through the mirror surface, the beam profile shall follow the expression q' we derive. So, at the interface where the collapsed region ends, there is a coupling efficiency between the field mode there and the fiber mode which is the one that we need.

We won't have a simplified expression for $\varepsilon(L, R, d)$ and there is no sense deriving that. Therefore we generate it's contour plot when $d = 0\mu m$ and $d = 100\mu m$, representing the one without the collapsed region and the one with a $100\mu m$ deep collapsed region.

A.2 Instruction for the program

The main structure of the program is supported by LabVIEW. For analyzing the position of the fiber, the program will call a corresponding python script to do the job. The camera control subVIs are not written by me but by Ackermann Automation. I simply downloaded them online and added them into my program. You can see an overview of the VI interface in figure A.1. You will find more detailed introduction of some frequently used panel

A.2. Instruction for the program

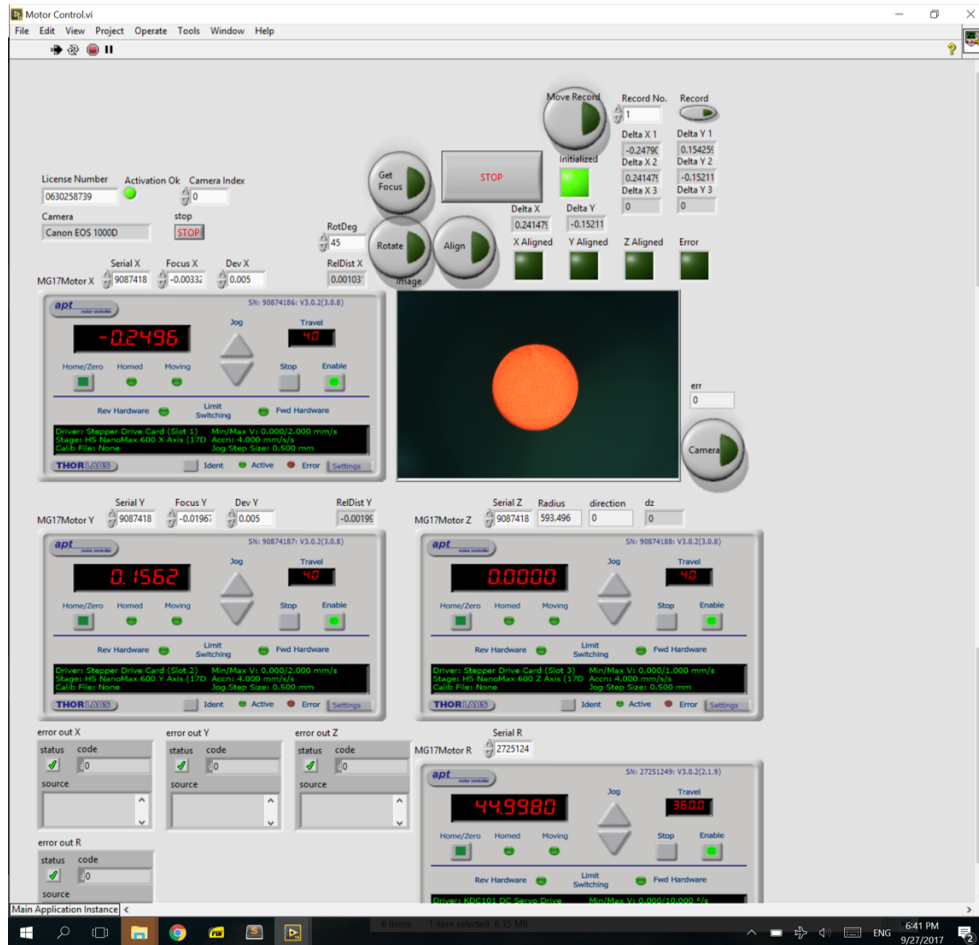


Figure A.1: Overview of the panel. The build-in APT interfaces are used for manually controlling the motorized stage. The screen with a fiber image is for viewing the captured image. The serial numbers for the motors were set as default values so there is no need to change them. You will find more detailed introduction for the other panel elements in figure A.2.

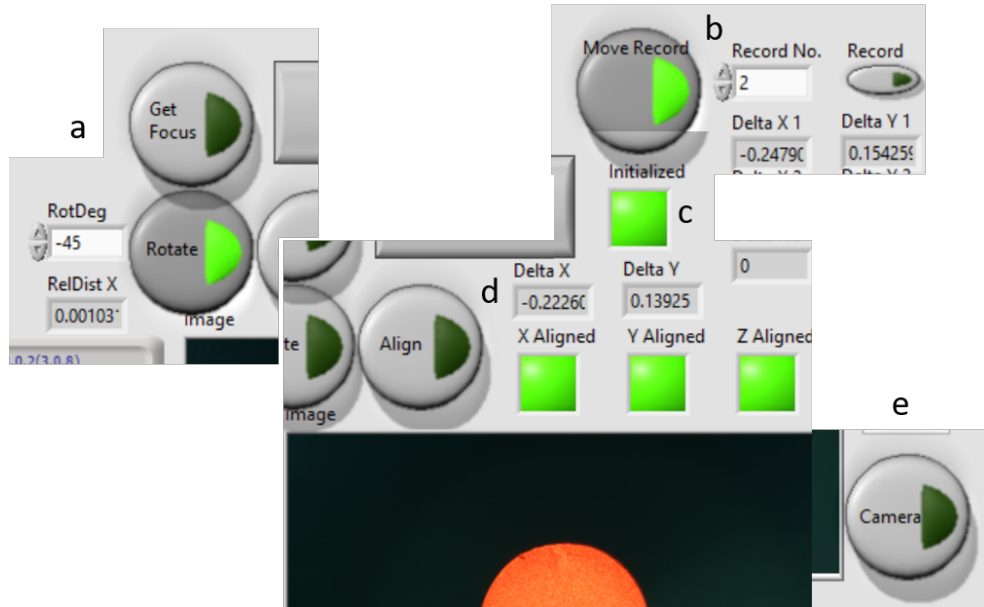


Figure A.2: The figure shown is divided into four sections. **a.** You can set the rotation angle here and by pressing the *Rotate* button the fiber is rotated by the angle you set. Above the *Rotate* button you will find a *Get Focus* button. It is used for determining the position of the CO₂ laser focus. It is recommended to update the focus as a daily routine. **b.** The *Record* button allows you to store the data, shown in *Delta X* and *Delta Y*, into *Delta X_i* and *Delta Y_i* determined by the *Record No.*. Later you could use the *Move Record* button to use the recorded distances to move the motors. If you are to implement the ablation method mentioned in section 2.3, you should record all the three sets of distances and later use the sets recorded to move the fiber. **c.** The *Initialized* pulb is used to indicate that the program is initialized and is ready to run operations. It is recommended not to touch anything before it lights up. **d.** The *Align* button allows you to align the fiber center (which the core locates) to the CO₂ laser focus you determined. During the process, the captured images are shown on the *image* screen. When the fiber is aligned, all the three *Aligned* pulbs will temporarily light up and the distance moved will be recorded in *Delta X* and *Delta Y*. **e.** The *Camera* button allows you to capture images when there is no task running.

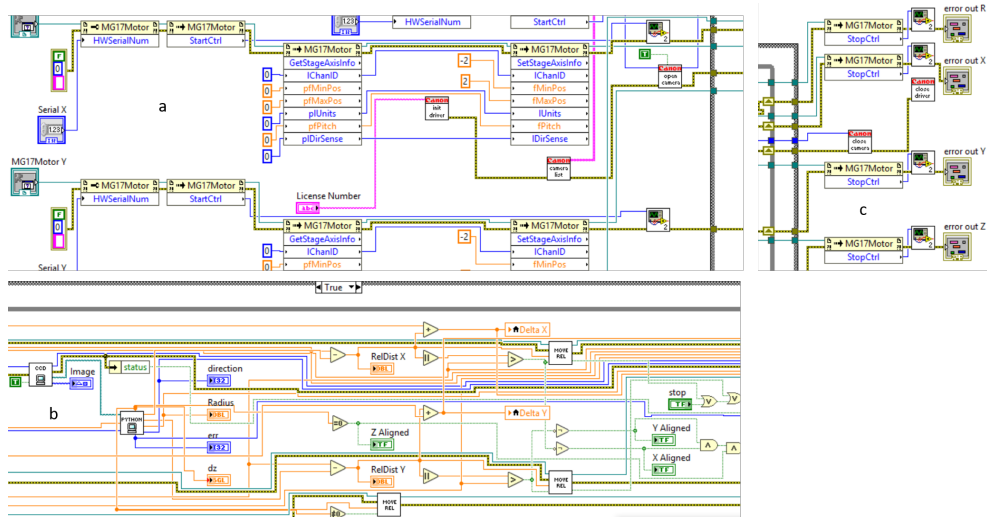


Figure A.3: The three main sections of the blockdiagram. To make the block-diagram more reader friendly, I use as many as subVIs to make it more clear. You will find the diagrams for most of the subVIs in figure A.4. **a.** The initializations of all the four motors and the camera control are completed here. **b.** The section to align the fiber to the CO₂ focus position. It is the most dense part of the program. **c.** The termination of all the four motors and the camera control are completed here.

elements in figure A.2.

If the reader wants to modify the program in the future, it is recommended to view figure A.3 and figure A.4 to get to know how the program is constructed. In the future, it is possible to modify the program to be less human cooperative.

A.3 Python codes used

A.3.1 To analyze the fiber tip surface

```
from PIL import Image
import numpy as np
import os
import glob
from skimage.restoration import unwrap_phase
from scipy.optimize import differential_evolution
#All the experiment parameters
wl=0.604#wavelength in um
pix=125/1550#the pixal scale to the real scale um
fibervec = [np.round(140/pix).astype(int),#x left
            np.round(260/pix).astype(int),#x right
            np.round(55/pix).astype(int),#y down]
```

A. APPENDIX

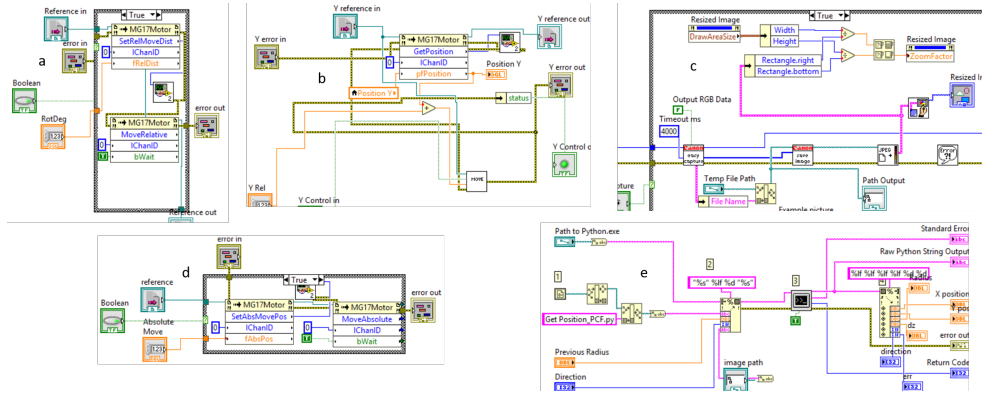


Figure A.4: Diagrams for the subVIs used in my program. **a.** The *Rotate* subVI used for rotating the motor based on the angle input by *RotDeg*. **b.** The *Move Rel* subVI is used to move the motor assigned based on the relative distance determined by *Y Rel*. The called *Move* subVI is described in **d.** **c.** The *CCD* subVI captures the image and outputs the image and its path. We were planning to use the CCD but end up using a Canon camera. That's why you can see the subVIs for Canon camera control in the subfigure. **d.** The *Move* subVI used to move the motor to the absolute position determined by *Absolute Move*. **e.** The *Python* subVI used for calling the Python script assigned through the Windows command line.

```

np.round(175/pix).astype(int)#y up
]
dimplevec = [np.round(170/pix).astype(int),#x left
             np.round(220/pix).astype(int),#x right
             np.round(100/pix).astype(int),#y down
             np.round(150/pix).astype(int)#y up
]
path=r"#The folder that stores the images
fname = sorted(glob.glob("%s*.jpg" % (path+os.sep)))
imgs=[]
for fname in fname:
    pic = Image.open(fname)
    imgs.append(np.flipud(np.array(pic).astype(float)))

phi=np.arctan((imgs[3][:,:,0]-imgs[1][:,:,0])/(imgs[0][:,:,0]-
             imgs[2][:,:,0]+0.001))#extract
             the phase of each pixal from the
             images
phicrop = phi[dimplevec[2]:dimplevec[3],dimplevec[0]:dimplevec[1]
]#cut out the dimple part
h=unwrap_phase(phicrop*2)/2*w1/(2*np.pi)/2#first reconstruct the
phase, then calculate the height
of each pixal

```

```

xfit, yfit = np.meshgrid(np.arange(h.shape[0])*pix,np.arange(h.
                             shape[1])*pix)
def gaussplane_DE(parameters,*data):
    mx,my,sigx,sigy,xG,yG,zt,Off=parameters
    x,y,z=data
    return np.sqrt(np.sum((Off+mx*x+my*y+zt*np.exp(-(((x-xG)/sigx
                                                    )**2+((y-yG)/sigy)**2))-z)**
                    2))
def gaussplane(x,y,mx,my,sigx,sigy,xG,yG,zt,Off):
    return Off+mx*x+my*y+zt*np.exp(-(((x-xG)/sigx)**2+((y-yG)/
                                                    sigy)**2))
fit = differential_evolution(gaussplane_DE,#fit the profile with
                             a 2D Gaussian function
                             [(-1,1), (-1,1),          # x- and y-
                                                    slope
                             (0,h.shape[0]*pix),      # sigx
                             (0,h.shape[1]*pix),      # sigy
                             (0,h.shape[0]*pix),      # x0
                             (0,h.shape[1]*pix),      # y0
                             (-3,3),                  # zt
                             (-1,1),                  # Offset
                             ],
                             args=(xfit.T,yfit.T,h))
bestfit = gaussplane(xfit,yfit,*fit.x)#fitted profile of the
                                     surface
#Then use what ever you like to plot the figures.

```

A.3.2 To determine the position of the core (quick but rough)

```

#!/usr/bin/env python
import sys
from PIL import Image
import numpy as np
import math
from matplotlib import pyplot as plt
from scipy.optimize import differential_evolution

pix=3.14/10000#Turn pixels into microns
offsetx=-0-(17-8)/17*3888*pix+0.039736#Calculate the focus
                                     position (x,y)
offsety=0-3.1/7*2592*pix-0.0479307
pic = Image.open(sys.argv[3])#Command Line Arguments are stored
                             in list argv
img=np.flipud(np.array(pic).astype(float))
xpx = img.shape[0]
ypx = img.shape[1]
err=0
halfb=np.amax(img[:, :,0])-3
if halfb<220:#If there is no laser spot on the image
    err=1
xavg=np.round(xpx/2).astype(int)
yavg=np.round(ypx/2).astype(int)

```

A. APPENDIX

```
count=0
xsum=0
ysum=0
xysum=0
tof=0
for i in range(xpx):
    for j in range(ypx):
        if img[i,j,0]>halfb:#Calculate the position of the core
            xsum=xsum+i*(img[i,j,0]-halfb)
            ysum=ysum+j*(img[i,j,0]-halfb)
            xysum=xysum+img[i,j,0]-halfb
            count=count+1
xavg=np.round(xsum/xysum).astype(int)
yavg=np.round(ysum/xysum).astype(int)
if count<2000:#In case what we get is actually a scattered light
    err=1
count=0
xsum=0
ysum=0
xysum=0

positionxp=yavg*pix+offsetx
positionyp=xavg*pix+offsety
positionx=1.022564*positionxp-0.03758*positionyp#Calibration
positiony=-0.00178*positionxp+0.9672*positionyp
radius=0
dz=0
direction=0
if err==1:
    positionx=0
```

A.3.3 To determine the position of the core (slow but accurate)

```
#!/usr/bin/env python
import sys
from PIL import Image
import numpy as np
import math
from matplotlib import pyplot as plt
from scipy.optimize import differential_evolution

pix=3.14/10000#Turn pixals into microns
offsetx=-0-(17-8)/17*3888*pix+0.039736#Calculate the focus
                                         position (x,y)
offsety=0-3.1/7*2592*pix-0.0479307
pic = Image.open(sys.argv[3])#Command Line Arguments are stored
                               in list argv
img=np.flipud(np.array(pic).astype(float))
xpx = img.shape[0]
ypx = img.shape[1]
err=0

halfb=np.amax(img[:, :, 0])-3
```

```

if halfb<220:#If there is no laser spot on the image
    err=1
dis=50#Reduce the pic resolution by #dis times to speed up the
fit

xavg=np.round(xpx/2).astype(int)
yavg=np.round(ypx/2).astype(int)
count=0
xsum=0
ysum=0
xysum=0
tof=0
for i in range(xpx):
    for j in range(ypx):
        if img[i,j,0]>halfb:#Calculate the position of the core
            xsum=xsum+i*(img[i,j,0]-halfb)
            ysum=ysum+j*(img[i,j,0]-halfb)
            xysum=xysum+img[i,j,0]-halfb
            count=count+1
#Roughly Get the position of the core
xavg=np.round(xsum/xysum).astype(int)
yavg=np.round(ysum/xysum).astype(int)
if count<2000:#In case what we get is actually a scattered light
    err=1
    count=0
    xsum=0
    ysum=0
    xysum=0

#Crop a small part of image containing the core
s=0#Because PCF is big
xbase=xavg-np.round(xpx/(2*(s+1))).astype(int)
ybase=yavg-np.round(ypx/(2*(s+1))).astype(int)
#Ensure the cropping frame is within the image
if xbase<0:
    xbase=0
if ybase<0:
    ybase=0
xfit, yfit = np.meshgrid(np.arange(xbase,xavg+np.round(xpx/(2*(s
+1))).astype(int)),np.arange(
ybase,yavg+np.round(ypx/(2*(s+1
))).astype(int)))
#Reduce the image resolution to speed up the fitting
h=np.zeros((np.round(xfit.shape[0]/dis).astype(int),np.round(xfit
.shape[1]/dis).astype(int)))

for i in range(h.shape[0]):
    for j in range(h.shape[1]):
        if xbase+i*dis<2592 and ybase+j*dis<3888:
            h[i,j]=img[xbase+i*dis,ybase+j*dis,0]
        else:
            h[i,j]=0
xfit,yfit=np.meshgrid(np.arange(h.shape[0])\
, np.arange(h.shape[1]))
#Define cost function (preventing scattering light)

```

```

def f_DE(parameters,*data):
    r0,x0,y0=parameters
    x,y,z=data
    sumn=0
    for i in range(z.shape[0]):
        for j in range(z.shape[1]):
            if (xfit[j,i]-x0)**2+(yfit[j,i]-y0)**2-r0**2>0:
                sumn=sumn+z[i,j]**2
            else:
                sumn=sumn+(255-z[i,j])**2*2
    return sumn
def f(x,y,r0,x0,y0):
    tempm=np.zeros(h.shape)
    for i in range(h.shape[0]):
        for j in range(h.shape[1]):
            if (xfit[j,i]-x0)**2+(yfit[j,i]-y0)**2-r0**2>0:
                tempm[i,j]=0
            else:
                tempm[i,j]=255
    return tempm
#Fit the data
fit = differential_evolution(f_DE,
                             [(0,600/dis),#r0
                              (h.shape[0]/4,h.shape[0]*3/4), #
                              (h.shape[1]/4,h.shape[1]*3/4), #
                              ], #
                             args=(xfit.T,yfit.T,h),
                             strategy='best1bin',
                             popsize=10
                             )
bestfit = f(xfit,yfit,*fit.x)

positionyp=(xbase+fit.x[1]*dis)*pix+offsety
positionxp=(ybase+fit.x[2]*dis)*pix+offsetx
positionx=1.022564*positionxp-0.03758*positionyp#Calibration
positiony=-0.00178*positionxp+0.9672*positionyp
radius=fit.x[0]*dis#Calculate the radius

```

A.3.4 To determine the size of the field beam (normal fibers)

```

#!/usr/bin/env python
import sys
from PIL import Image
import numpy as np
import math
from matplotlib import pyplot as plt
from scipy.optimize import differential_evolution

pix=1.15/10000
offsetx=-0-(17-8)/17*3888*pix
offsety=0-2.5/7*2592*pix

```

```

pic = Image.open(sys.argv[3])#Command Line Arguments are stored
                                in list argv
img=np.flipud(np.array(pic).astype(float))
xpx = img.shape[0]
ypx = img.shape[1]
bfrac=0.9
halfb=np.amax(img[:, :, 0])-3
dis=40#Reduce the image resolution
radiusthreshold=500#In case the radius is small enough
radiusslope=0.0012
radiusteststep=0.07#Testing step size
previousradius=float(sys.argv[1])
direction=int(sys.argv[2])#Moving direction
dz=0#Moving value
xavg=np.round(xpx/2).astype(int)
yavg=np.round(ypx/2).astype(int)
count=0
xsum=0
ysum=0
xysum=0
tof=0
for i in range(xpx):
    for j in range(ypx):
        if img[i,j,0]>halfb:
            xsum=xsum+i
            ysum=ysum+j
            xysum=xysum+1
            count=count+1
#Get the position of the core
xavg=np.round(xsum/xysum).astype(int)
yavg=np.round(ysum/xysum).astype(int)

count=0
xsum=0
ysum=0
xysum=0
#Crop a small part of image containing the core
s=1
xbase=xavg-np.round(xpx/(2**(s+1))).astype(int)
ybase=yavg-np.round(ypx/(2**(s+1))).astype(int)
#Ensure the cropping frame is within the image
if xbase<0:
    xbase=0
if ybase<0:
    ybase=0
xfit, yfit = np.meshgrid(np.arange(xbase,xavg+np.round(xpx/(2**(s
+1))).astype(int)),np.arange(
ybase,yavg+np.round(ypx/(2**(s+1
))).astype(int)))

h=np.zeros((np.round(xfit.shape[0]/dis).astype(int),np.round(xfit
.shape[1]/dis).astype(int)))
#Reduce the image resolution to speed up the fitting
for i in range(h.shape[0]):

```

```

    for j in range(h.shape[1]):
        if xbase+i*dis<2592 and ybase+j*dis<3888:
            h[i,j]=img[xbase+i*dis,ybase+j*dis,0]
        else:
            h[i,j]=0
xfit,yfit=np.meshgrid(np.arange(h.shape[0])\
                      ,np.arange(h.shape[1]))
#Define cost function (preventing scattering light)
def f_DE(parameters,*data):
    r0,x0,y0=parameters
    x,y,z=data
    sumn=0
    for i in range(z.shape[0]):
        for j in range(z.shape[1]):
            if (xfit[j,i]-x0)**2+(yfit[j,i]-y0)**2-r0**2>0:
                sumn=sumn+z[i,j]**2
            else:
                sumn=sumn+(255-z[i,j])**3*3
    return sumn
def f(x,y,r0,x0,y0):
    tempm=np.zeros(h.shape)
    for i in range(h.shape[0]):
        for j in range(h.shape[1]):
            if (xfit[j,i]-x0)**2+(yfit[j,i]-y0)**2-r0**2>0:
            else:
                tempm[i,j]=255
    return tempm
#Fit the data
fit = differential_evolution(f_DE,
                             [(0,600/dis),#r0
                              (h.shape[0]/4,h.shape[0]*3/4), #
                              (h.shape[1]/4,h.shape[1]*3/4), #
                              ],
                             args=(xfit.T,yfit.T,h),
                             strategy='best1bin',
                             popsize=10)

positionx=((ybase+fit.x[2]*dis)*pix+offsetx-0.0544*((xbase+fit.x[
1]*dis)*pix+offsety))/(1-0.112*0.0544)
positiony=((xbase+fit.x[1]*dis)*pix+offsety-0.112*((ybase+fit.x[2
]*dis)*pix+offsetx))/(1-0.112*0.0544)
radius=fit.x[0]*dis#Calculate the radius
if radius<radiusthreshold:
    dz=0
else:
    if direction==0:
        dz=radiusteststep
        direction=1
    elif radius>previousradius:
        direction=-direction

```

A.3. Python codes used

```
        dz=(radius-radiusthreshold+5)*radiusslope*direction
    else:
        dz=(radius-radiusthreshold+5)*radiusslope*direction
    print (positionx,positiony,radius,dz,direction,sep=" ")#)
```

Bibliography

- [1] Julia Benedikter, Thomas Hümmer, Matthias Mader, Benedikt Schleder, Jakob Reichel, Theodor W Hänsch, and David Hunger. Transverse-mode coupling and diffraction loss in tunable fabry-pérot microcavities. *New Journal of Physics*, 17(5):053051, 2015.
- [2] Andreas Bick, Christina Staarmann, Philipp Christoph, Ortwin Hellmig, Jannes Heinze, Klaus Sengstock, and Christoph Becker. The role of mode match in fiber cavities. *Review of Scientific Instruments*, 87(1):013102, 2016.
- [3] Birgit Brandstätter, Andrew McClung, Klemens Schüppert, Bernardo Casabone, Konstantin Friebe, Andreas Stute, Piet O Schmidt, Christian Deutsch, Jakob Reichel, Rainer Blatt, et al. Integrated fiber-mirror ion trap for strong ion-cavity coupling. *Review of Scientific Instruments*, 84(12):123104, 2013.
- [4] Yves Colombe, Daniel H. Slichter, Andrew C. Wilson, Dietrich Leibfried, and David J. Wineland. Single-mode optical fiber for high-power, low-loss uv transmission. *Opt. Express*, 22(16):19783–19793, Aug 2014.
- [5] Lukas Greuter, Sebastian Starosielec, Daniel Najer, Arne Ludwig, Luc Duempelmann, Dominik Rohner, and Richard J Warburton. A small mode volume tunable microcavity: development and characterization. *Applied Physics Letters*, 105(12):121105, 2014.
- [6] Lukas Emanuel Greuter. *Self-assembled quantum dots in a fully tunable microcavity*. PhD thesis, University of Basel, 2015.
- [7] Gurpreet Kaur Gulati, Hiroki Takahashi, Nina Podoliak, Peter Horak, and Matthias Keller. Fiber cavities with integrated mode matching optics. *arXiv preprint arXiv:1703.03785*, 2017.

- [8] David Hunger, Christian Deutsch, Russell J Barbour, Richard J Warburton, and Jakob Reichel. Laser micro-fabrication of concave, low-roughness features in silica. *AIP Advances*, 2(1):012119, 2012.
- [9] David Hunger, Tilo Steinmetz, Yves Colombe, Christian Deutsch, Theodor W Hänsch, and Jakob Reichel. A fiber fabry-perot cavity with high finesse. *New Journal of Physics*, 12(6):065038, 2010.
- [10] H. J. Kimble. The quantum internet. *Nature*, 453(7198):1023–1030, Jun 2008.
- [11] Jonathan C Knight. Photonic crystal fibres. *nature*, 424(6950):847, 2003.
- [12] W. Nagourney. *Quantum Electronics for Atomic Physics and Telecommunication*. Oxford graduate texts. Oxford University Press, 2014.
- [13] Krzysztof M. Nowak, Howard J. Baker, and Denis R. Hall. Analytical model for co2 laser ablation of fused quartz. *Appl. Opt.*, 54(29):8653–8663, Oct 2015.
- [14] Konstantin Ott, Sebastien Garcia, Ralf Kohlhaas, Klemens Schüppert, Peter Rosenbusch, Romain Long, and Jakob Reichel. Millimeter-long fiber fabry-perot cavities. *Optics express*, 24(9):9839–9853, 2016.
- [15] NKT Photonics. Fiber handling, stripping, cleaving and coupling. 2009.
- [16] Stephan Ritter, Christian Nolleke, Carolin Hahn, Andreas Reiserer, Andreas Neuzner, Manuel Uphoff, Martin Mücke, Eden Figueroa, Joerg Bochmann, and Gerhard Rempe. An elementary quantum network of single atoms in optical cavities. *Nature*, 484(7393):195–200, Apr 2012.
- [17] Philip Russell. Photonic crystal fibers. *science*, 299(5605):358–362, 2003.
- [18] Hiroki Takahashi, Jack Morphew, Fedja Oručević, Atsushi Noguchi, Ezra Kassa, and Matthias Keller. Novel laser machining of optical fibers for long cavities with low birefringence. *Optics express*, 22(25):31317–31328, 2014.
- [19] Haruka Tanji-Suzuki, Ian D Leroux, Monika H Schleier-Smith, Marko Cetina, Andrew T Grier, Jonathan Simon, and Vladan Vuletic. Interaction between atomic ensembles and optical resonators: classical description. *arXiv preprint arXiv:1104.3594*, 2011.
- [20] Chi Wang, Fang Zhang, Shu-Bo Bi, Xue-Qin Xia, and Ting-Ting Xu. Fabrication method of ultra-small gradient-index fiber probe. *Advances in Manufacturing*, 2(4):327–332, Dec 2014.
- [21] Amnon Yariv. *Quantum electronics*. Wiley, 1989.



Eidgenössische Technische Hochschule Zürich
Swiss Federal Institute of Technology Zurich

Declaration of originality

The signed declaration of originality is a component of every semester paper, Bachelor's thesis, Master's thesis and any other degree paper undertaken during the course of studies, including the respective electronic versions.

Lecturers may also require a declaration of originality for other written papers compiled for their courses.

I hereby confirm that I am the sole author of the written work here enclosed and that I have compiled it in my own words. Parts excepted are corrections of form and content by the supervisor.

Title of work (in block letters):

Authored by (in block letters):

For papers written by groups the names of all authors are required.

Name(s):

First name(s):

With my signature I confirm that

- I have committed none of the forms of plagiarism described in the '[Citation etiquette](#)' information sheet.
- I have documented all methods, data and processes truthfully.
- I have not manipulated any data.
- I have mentioned all persons who were significant facilitators of the work.

I am aware that the work may be screened electronically for plagiarism.

Place, date

Signature(s)

For papers written by groups the names of all authors are required. Their signatures collectively guarantee the entire content of the written paper.